HURRICANE INDUCED WAVE AND SURGE FORCES ON BRIDGE DECKS

A Thesis

by

RONALD LEE MCPHERSON

Submitted to the Office of Graduate Studies of
Texas A&M University
in partial fulfillment of the requirements for the degree of

MASTER OF SCIENCE

August 2008

Major Subject: Ocean Engineering

HURRICANE INDUCED WAVE AND SURGE FORCES ON BRIDGE DECKS

A Thesis

by

RONALD LEE MCPHERSON

Submitted to the Office of Graduate Studies of
Texas A&M University
in partial fulfillment of the requirements for the degree of

MASTER OF SCIENCE

Approved by:

Chair of Committee,	Billy L. Edge
Committee Members,	James Kaihatu
	Alejandro Orsi
Head of Department,	David Rosowsky

August 2008

Major Subject: Ocean Engineering

ABSTRACT

Hurricane Induced Wave and Surge Forces on Bridge Decks.

(August 2008)

Ronald Lee McPherson, B.S., Texas A&M University

Chair of Advisory Committee: Dr. Billy L. Edge

The damaging effects of hurricane landfall on U.S. coastal bridges have been studied using physical model testing. Hurricane bridge damage and failure susceptibility has become very evident, especially during hurricane seasons 2004 and 2005 in the Gulf of Mexico. The combination of storm surge and high waves caused by a hurricane can produce substantial loads on bridge decks leading to complete bridge failure. Several theoretical methods have been developed to estimate these forces but have not been tested in a laboratory setting for a typical bridge section. Experiments were done using a large-scale 3-D wave basin located at the Haynes Coastal Engineering Laboratory at Texas A&M University to provide estimates of the horizontal and vertical forces for several conditions to compare with the forces predicted with the existing models. The wave force results show no strong correlation between the actual force measured and the predicted force of existing theoretical methods. A new method is derived from the existing theoretical methods. This model shows a strong correlation with both the measured horizontal and vertical forces.

To my mother, father, family, and adored wife, Lauren.

ACKNOWLEDGEMENTS

There are several people I would like to acknowledge for their assistance in completing this research. I would like to extend my sincere gratitude to Dr. Billy Edge for his support and direction in all of my graduate studies. I would also like to express my thanks to Oscar and Carmen Cruz-Castro for their assistance in running tests, as well as their invaluable guidance and support in creating accurate physical model tests. Also, I would like to thank Dr. Kaihatu and Dr. Orsi for serving as committee members. I would like to acknowledge the support of the Federal Highway Administration as well as several state transportation departments for specific knowledge. Also, the forensic information obtained by several firms and institutions following the 2004 and 2005 hurricane seasons is greatly appreciated.

TABLE OF CONTENTS

LIST OF FIGURES

Page

Page

Page

LIST OF TABLES

CHAPTER I

INTRODUCTION

Background

Hurricanes can generate forces which cause hydraulically induced failure in coastal bridges. This was especially apparent in the recent hurricanes: Ivan and Katrina. The predominant mechanisms that cause failure on bridge decks during a hurricane are surge and waves. Figure 1-1 shows U.S. Highway 90 crossing the Biloxi Bay in Mississippi after Hurricane Katrina. In the foreground of the image, the short bridge height allows the bridge decks to be subjected to surge and waves. The bridge decks in this section are completely displaced. In the background of the image, the bridge height increases to allow passage for large boats.

Figure 1- 1 U.S. Highway 90 over Biloxi Bay after Hurricane Katrina (Douglass et al. 2006)

This thesis follows the style of *Journal of Waterway, Port, Coastal and Ocean Engineering*.

This section of the bridge was only subjected to the winds of the hurricane and experienced no bridge deck displacement.

Numerous bridges have failed during hurricanes. Of the recent hurricanes: Ivan and Katrina, the notable bridges that have experienced damage include the I-10 bridge across Escambia Bay, the I-10 bridge across Lake Pontchartrain, the U.S. 90 bridges across the Biloxi Bay and Bay of St. Louis, and the on ramp to the I-10 bridge across Mobile Bay (Douglass et al. 2006). During Hurricane Katrina alone, 44 bridges experienced damage (Padgett et al. 2008).

During a hurricane event, the sustained strong winds essentially blow water up against the coast causing the water level to rise above the normal water level (Dean and Dalrymple 2002). This rise in water level is termed "surge". According to Dean and Dalrymple, there are several contributors to the total surge experienced during a storm event. These include: barometric tide, wind stress tide, and Coriolis tide. Of these, wind stress tide is the dominant contributor to the total surge during a storm.

The width and depth of a shelf adjacent to a shoreline is an important contributor to the severity of surge during a storm event. A classic example of this is Hurricane Katrina. The continental shelf in the Gulf of Mexico is relatively wide and shallow especially when compared to Hawaii and the Atlantic side of Florida. Surge is inversely proportional to water depth and therefore as the water depth decreases the surge increases (Dean and Dalrymple 2002). As Hurricane Katrina traveled across the wide shallow continental shelf, the surge continued to increase for the length of the shelf resulting in surge exceeding 20 ft in some areas (Douglass et al. 2006). In locations with little or no

shelf, less of the water column is affected by the wind. Thus, these locations experience smaller surge.

The other predominant damaging mechanism that causes bridge failure is wave induced loads. During storm events waves become significantly larger. When accompanied by an increased water level, the waves are then able to come into contact with the structure. This is shown in Figure 1-2. The energy carried by the waves is then partially transferred to the structure. This combined with buoyancy can cause the bridge to fail.

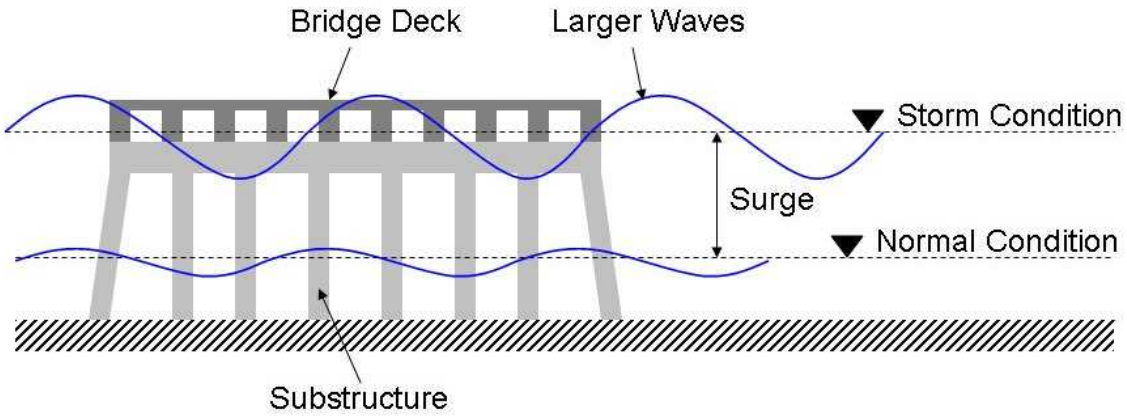

Figure 1- 2 Schematic of bridge deck subject to surge and waves during storm conditions

Purpose

There are several methods of estimating the forces applied to bridge decks; however they are based on unverified theoretical or empirical methods. Currently there has been little experimental work done to estimate the forces subjected to coastal bridge decks (Cruz-Castro et al. 2006). Structures other than bridges such as piers and platforms are subject to wave forces with and without surge and have been the subject of a great

deal of research. This previous research is valuable to the present because of the wave loading on similar horizontal deck geometries. However, this work does not include experiments with the structure submerged. The transportation community does not have adequate design tools to prevent the devastating effects of bridge failure due to hurricane conditions. Moreover, there is no agreed upon method to appropriately estimate the forces a coastal bridge will endure from wave and surge conditions during a hurricane (Cruz-Castro et al 2006).

The reason for bridge deck displacement has been widely agreed upon as the combination of an upward force (vertical force) and lateral force (horizontal force). However, specific mechanisms such as buoyancy caused by air-entrapment and quantifiable horizontal and vertical forces are still in debate. To better understand these mechanisms, a physical model was constructed in the Haynes Coastal Engineering Laboratory at Texas A&M to test forces on bridge decks caused by both waves and surge. The physical model was subjected to several combinations of water depths and wave heights as well as different types of waves. The forces and moments experienced by the physical model as well as wave conditions at various locations during the tests were measured. From this information forces and moments can be broken down in to components (x, y, z) and analyzed in detail and compared with previous theoretical methods.

The ultimate goal of this research is to quantify the forces on a bridge deck given a known wave and surge condition. Preexisting research on hurricanes can provide information on possible wave conditions near coastal bridges for past storms or potential storms. With this information, force estimations can be made for actual coastal bridges.

These estimations can be used several ways including post-storm damage investigations, pre-storm damage predictions, retro-fit coastal bridge design, and new coastal bridge design. Where preexisting information is not known, it may be necessary to hind-cast surge and wave conditions, much like is being done for coastal Louisiana and Mississippi.

CHAPTER II

PREVIOUS LITERATURE

Wave forces on highway bridge decks have only recently been a topic of interest in engineering literature. Therefore there is limited information relating directly to highway bridges. However, various nearshore and offshore structures with similar geometries such as piers and offshore platforms have received a substantial amount of attention. This body of information has a large potential of application to wave forces on highway bridge decks. The following are summaries of various literatures found to be relevant to the subject material and have developed some form of theoretical model to estimate wave forces on deck-like structures. Sarpkaya and Isaacson (1981) and others have presented detailed descriptions of the effects of wave forces in general. Much of the work has been focused on piles or slender structural elements for platforms but there has been little information related to vertical uplift forces on complex geometries.

Kaplan (1992) and Kaplan et al. (1995)

Kaplan, in the 1992 Offshore Technology Conference proceedings, discusses a theoretical approach to time histories of wave impact forces on offshore decks. Kaplan focuses on impact forces on vertical circular cylinders and vertical forces on flat plates. Kaplan in 1995 Offshore Mechanics and Artic Engineering conference proceedings further develops the theory by adding more applications such as horizontal wave forces on cross members.

Kaplan uses a combination of momentum change and drag effects to estimate wave forces on the various offshore platform members. The inertia term of the vertical force is derived by taking the time derivative of the product of the three-dimensional added mass of a flat plate and the vertical velocity. The drag term of the vertical force is found in the same manner as developed by Morrison 1950. Equation (2-1) and (2-2) are the vertical force equations condensed and expanded, respectively.

$$F_z = \frac{\partial}{\partial t}(M_3 w) + \frac{\rho}{2} b l C_D w|w| \tag{2-1}$$

$$= \rho\frac{\pi}{8} b \frac{l^2}{\left[1+\left(\frac{l}{b}\right)^2\right]^{1/2}} \dot{w} + \rho\frac{\pi}{4} b l \frac{dl}{dt} \frac{1+\frac{1}{2}\left(\frac{l}{b}\right)^2}{\left[1+\left(\frac{l}{b}\right)^2\right]^{1/2}} w + \frac{\rho}{2} b l C_D w|w| \tag{2-2}$$

M_3 is defined as the three-dimensional added mass of the flat plate. This is defined in Equation (2-3).

$$M_3 = \rho\frac{\pi}{8} \frac{b l^2}{\left[1+\left(\frac{l}{b}\right)^2\right]^{1/2}} \tag{2-3}$$

The terms l and $\frac{dl}{dt}$ represent the horizontal deck wetted length and time rate of change of the deck wetted length. $\frac{dl}{dt}$ can be represented by the wave celerity while the wave crest is traveling along the length of the horizontal deck y. After the wave has reached the end of the deck the $\frac{dl}{dt}$ term retains a value of zero.

The theory presented in Kaplan et al. 1995 was compared to preexisting experimental research. The comparisons were represented by bias, defined as the ratio of measured force and theoretical force. Horizontal force from one data set was compared to theory, and the bias varied from 0.92 to 1.26. Also, both horizontal and vertical force from another data set was compared to theory. The horizontal force bias varied from 0.79 to 1.23, and the vertical force bias varied from 0.63 to 1.46.

Bea et al. (2001)

Bea et al. discusses wave crest forces on the lower decks of offshore platforms. It is stated that the extreme condition storm wave would be higher than the lower deck of many older platforms. By using the American Petroleum Institute (API) wave force guidelines, it was found that most platforms would not survive the extreme storm condition. An analytical solution is used to re-qualify several platforms subject to possible inundating storm wave crests. The analytical solution is an application and modification of the equations developed by Morrison 1950. The total force "imposed" on the platform is given in Equation (2-4).

$$Ftw = Fb + Fs + Fd + Fl + Fi \qquad (2\text{-}4)$$

Where *Fb* is the buoyancy force (vertical), *Fs* is the slamming force, *Fd* is the drag force (horizontal), *Fl* is the lift force (vertical), and *Fi* is the inertial force.

The horizontal slamming force is defined as follows:

$$Fs = 0.5C_s \rho A u^2 \tag{2-5}$$

Where ρ is the mass density of seawater, A is the vertical deck area subject to wave crest, u is the horizontal fluid velocity in the wave crest, and C_s is the coefficient of slamming which can vary from $C_s=\pi$ to $C_s=2\pi$. An "effective" slamming force is also discussed which uses a dynamic load factor coefficient, Fe which reduces the slamming force evaluated from Equation (2-5) by:

$$Fs' = FeFs \tag{2-6}$$

The inundation forces are developed as well. The horizontal drag force using the drag coefficient, C_d is given in Equation (2-7).

$$Fd = 0.5\rho C_d A u^2 \tag{2-7}$$

The vertical lift force is given in Equation (2-8).

$$Fl = 0.5\rho C_l A u^2 \tag{2-8}$$

C_l is defined as the lift coefficient. The forces in the vertical direction are not discussed in detail because the platforms under investigation have open or grated floors. These floors have shown to incur significantly less vertical force than horizontal force.

The inertial force is given in Equation (2-9).

$$Fi = \rho C_m V a \qquad (2\text{-}9)$$

Where V is the volume of deck inundated, a is the water acceleration, and C_m is the inertia coefficient.

Field experience is also presented in the literature. Damage incurred to platforms affected by Hurricanes Andrew, Roxanne, Camille, and Hilda is discussed. A "good" correlation is found between damage and "green water" exposed to the lower decks of the platforms.

Laboratory results from Finnigan and Petrauskas were used to compare the API and modified procedures. Statistical information, including mean, standard deviation and coefficient of variance is given in terms of bias (ratio of measured maximum horizontal force to analytical maximum horizontal force). Certain test setups show promising results with mean bias close to 1 while other setups show bias reaching 2+.

Tirindelli et al. (2002)

Tirindelli et al. (2002) reviews existing methods for evaluating wave loads on exposed jetties and related structures. Flume tests to measure wave induced forces on beam and deck structures were carried out at H. R. Wallingford. A 1:25 scale model of a jetty was used in three different configurations: panels, no panels, and flat plate. The panel configuration is designed to eliminate three-dimensional effects as the wave inundates the structure. The no panel configuration is designed to simulate an actual jetty of similar geometry. The three configurations are shown in Figure 2-1.

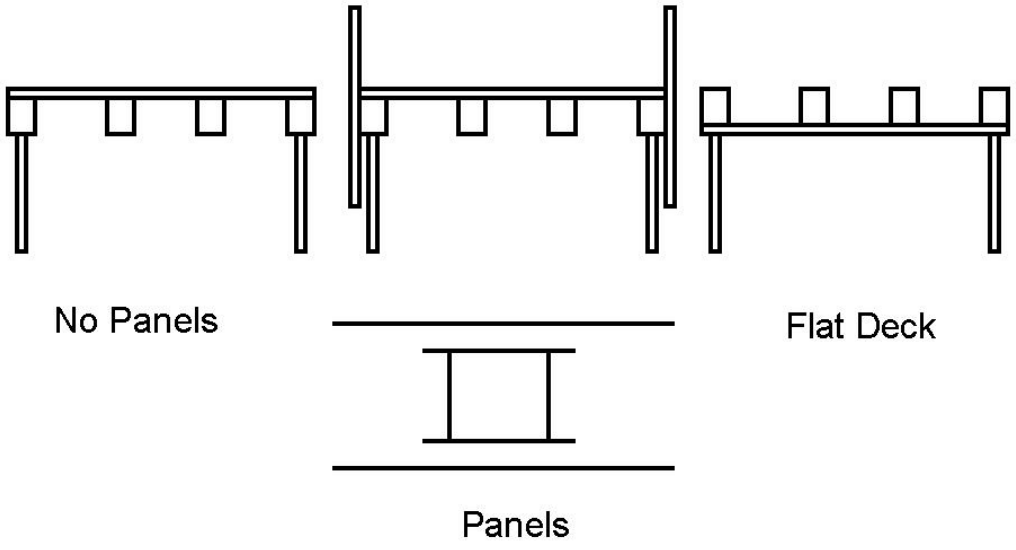

Figure 2- 1 H. R. Wallingford test configurations

The specimen has four testing elements built in which measure pressure on an exterior beam, interior beam, exterior deck, and interior deck.

Of the data collected, the horizontal and vertical forces were compared to significant wave height. It was shown that both horizontal and vertical forces increased as significant wave height increased. There was no discernable difference between the test configurations for the horizontal force. It was observed that after ignoring a few outliers the vertical force for both beam and deck increased in a linear fashion where the uplift force depended on the element size and not shape.

The existing models by Kaplan (1992) and Shih & Anastasiou (1992) were compared to the exterior deck element. The downward forces were also compared to the Kaplan model. In general, both the Kaplan and Shih models under predicted the magnitude of the uplift force. The Kaplan model also under predicted the magnitude of the downward forces.

McConnell et al. (2004)

McConnell et al. (2004) is a comprehensive literature survey that covers many aspects of hydraulic loading on piers and jetties exposed to "green water". Within the literature review a different approach for quantifying vertical and horizontal wave crest loads on structures using the experimental data from H. R. Wallingford is presented. The design structure under investigation was the same jetty used in Tirindelli (2002). The experiments were done in a wave flume with modern wave-generation capabilities. A typical loading found by the experiments show a slow-varying load that corresponds to the period of the wave and a short duration impact load when the wave first hits the structure.

The analytical method used to estimate the forces is based on a hydrostatic approach. Individual components of the jetty (seaward beam, internal beam, and internal deck) are calculated separately and later added together to find a total force. The "base vertical force", F_v^* is found by multiplying the pressure under the component by the projected area of the component in the horizontal plane. The pressure is defined by the difference in the elevation of the maximum wave crest and the elevation of the bottom of the deck. The "base horizontal force", F_h^* is found similarly by multiplying the pressure of the component face (vertical plane) by its area. The pressure is defined by the difference in the elevation of the maximum wave crest and the centroid of the component face. The "base vertical force" and "base horizontal force" are demonstrated in Figure 2-2.

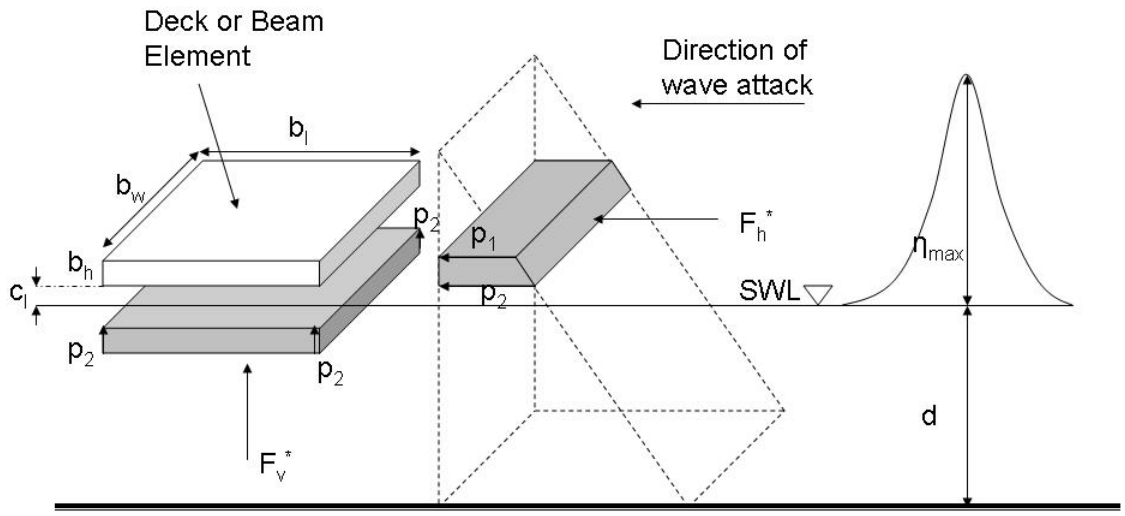

Figure 2- 2 Schematic of vertical and horizontal force applied to a deck or beam element

The equations for the basic wave forces are as follows:

$$F_v^* = b_w b_l p_2 \tag{2-10}$$

$$F_h^* = b_w(\eta_{\max} - c_l)\frac{p_2}{2} \quad \text{for } \eta_{max} \le c_l + b_h \tag{2-11}$$

$$F_h^* = b_w b_h \frac{(p_1 + p_2)}{2} \text{ for } \eta_{max} > c_l + b_h \tag{2-12}$$

From the basic force parameters F_v^* and F_h^*, a quasi-static force parameter is defined. Figure 2-3 demonstrates the quasi-static force parameter during a typical force loading.

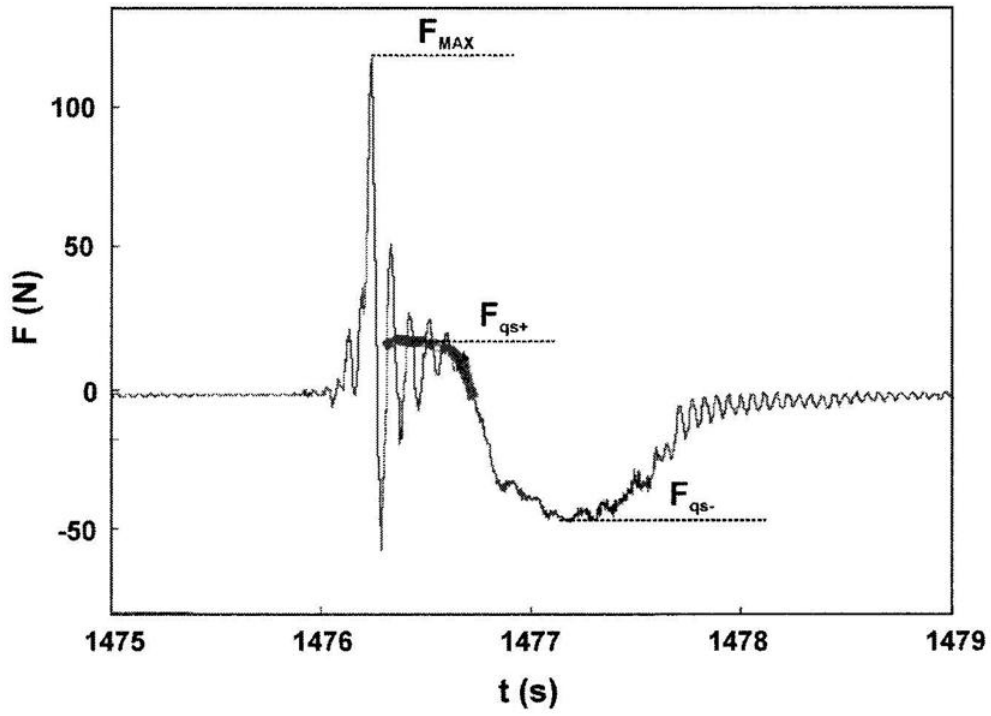

Figure 2- 3 Definition of quasi-static force parameters (Kerenyi 2005)

The equation for the quasi-static force is given as:

$$\frac{F_{qs}}{F^*} = \frac{a}{\left[\frac{\left(\eta_{\max} - c_l\right)}{H}\right]^b} \tag{2-13}$$

Where F_{qs} is the quasi-static force, F^* is the basic wave force (vertical or horizontal), c_l is the clearance defined in Figure 2-2, H is the wave height, η_{max} is the maximum wave crest elevation relative to the SWL, and the coefficients a and b are empirical.

The empirical coefficients a and b differ for each element, upward and downward loading, and vertical and horizontal forces. These coefficients are given in Table 2-1.

Table 2- 1 Coefficients defined by McConnell et al. 2004 for evaluating the quasi-static forces for beam and deck elements

Wave Load and Configuration	a	b
Upward vertical forces (seaward beam and deck)	0.82	0.61
Upward vertical forces (internal beam only)	0.84	0.66
Upward vertical forces (internal deck, 2D and 3D effects)	0.71	0.71
Downward vertical forces (seaward beam and deck)	-0.54	0.91
Downward vertical forces (internal beam only)	-0.35	1.12
Downward vertical forces (internal deck, 2D effects)	-0.12	0.85
Downward vertical forces (internal deck, 3D effects)	-0.80	0.34
Shoreward horizontal forces, F_{hqs+} (seaward beam)	0.45	1.56
Shoreward horizontal forces, F_{hqs+} (internal beam)	0.72	2.30
Seaward horizontal forces, F_{hqs-} (seaward beam)	-0.20	1.09
Seaward horizontal forces, F_{hqs-} (internal beam)	-0.14	2.82

Douglass et al. (2006)

Douglass, at the University of South Alabama, uses a similar method to the McConnell approach, however this method is simplified. The area of interest of the literature is U.S. Highway bridge decks. Douglass et al. (2006) uses the same hydrostatic approach as McConnell but does not separate the structure into various components.

The "reference" vertical force, F_v^* of the entire bridge is found by multiplying the pressure under the bridge deck by its projected area in the horizontal plane. The pressure is found by taking product of gravity, density, and the difference of the maximum elevation of the wave crest and the elevation of the bottom of the deck. The estimated

vertical force, F_v is then found by multiplying the "reference" vertical force by an empirical coefficient for a varying load, $C_{v\text{-}va}$. This is shown in Equations (2-14) and (2-15).

$$F_v^* = \gamma(\Delta Z_v)A_v \quad (2\text{-}14)$$

$$F_v = c_{v-va}F_v^* \quad (2\text{-}15)$$

The "reference" horizontal force is found by multiplying the pressure and area of the vertical face of the bridge. The pressure is found by taking the product of gravity, density, and the difference in the maximum elevation of the wave crest and centroid elevation of the bridge front face The estimated horizontal force, F_h is then found by multiplying the "reference" horizontal force, F_h^* with an empirical coefficient for a varying load, $c_{h\text{-}va}$ and a reduction empirical coefficient, c_r that takes in to account the number of girders on the deck, N. This is shown in Equations (2-16) and (2-17).

$$F_h^* = \gamma(\Delta Z_h)A_h \quad (2\text{-}16)$$

$$F_h = \left[1 + c_r(N-1)\right]c_{h-va}F_h^* \quad (2\text{-}17)$$

Figure 2-4 is a definition sketch for ΔZ_h, ΔZ_v, A_h, A_v, and η_{max} of the hydraulic loads on a bridge deck.

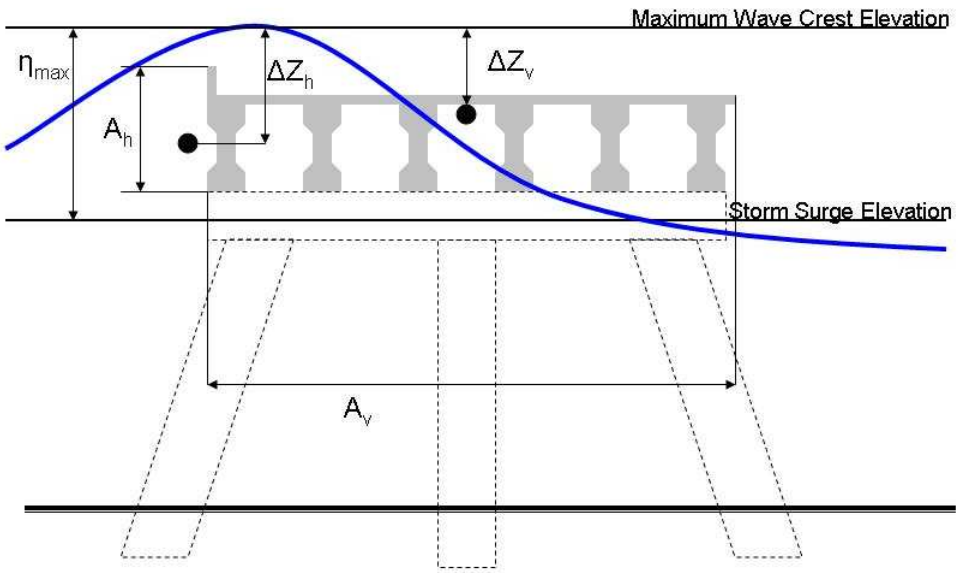

Figure 2- 4 Definition sketch for the Douglass method

CHAPTER III

RESEARCH METHODOLOGY

Several experiments were completed to investigate forces caused by various combinations of surge and waves on a physical model. Wave and force measurements as well as observational data were recorded. Several sets of experiments were completed for this research. In each set of experiments a variety of parameters were tested such as water depth, period, wave height, and wave type on a particular physical model. After each set of experiments, the recorded data were analyzed. Due to the progressive nature of research, the test setup for each set of experiments was usually enhanced in an effort to create a more accurate test.

Facility

The only testing facility used during the research was the Haynes Coastal Engineering Laboratory at Texas A&M University. The facility contains a shallow water 3-D basin equipped with a 48 paddle servo-powered wave generator. The paddles are independently driven allowing the wave generator to create a large array of waves including (but not limited to): monochromatic, nonlinear, solitary, multidirectional, and spectral (i.e. TMA and JONSWAP). A rock beach lines the opposite wall of the wave generator which dissipates a majority of the wave energy reducing undesirable wave reflection. While the basin is capable of producing a current in conjunction with waves, this feature was not utilized since the damaging mechanisms under investigation included only surge and waves. Figure 3-1 shows a 3-D rendering of the facility.

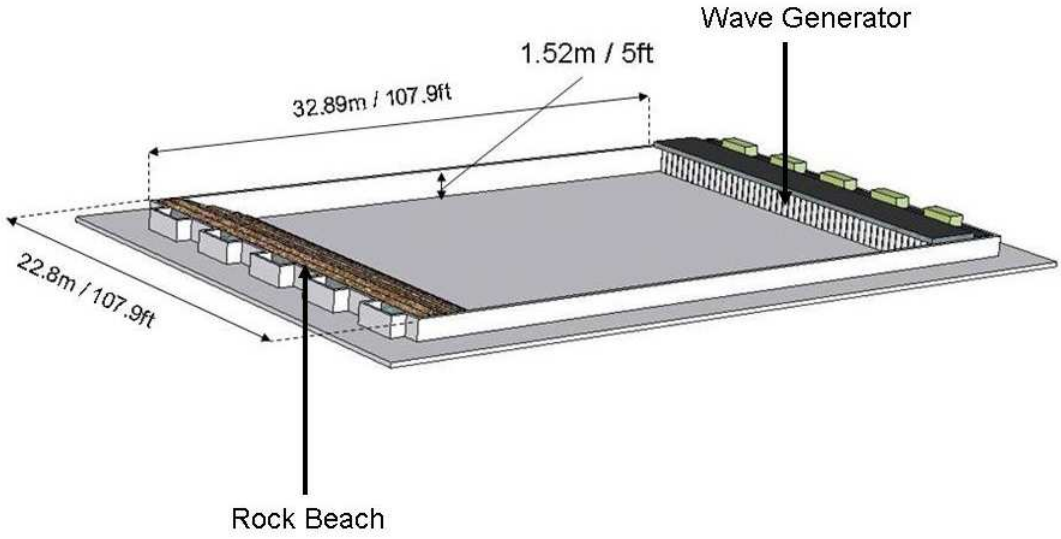

Figure 3- 1 Haynes Coastal Engineering Laboratory 3-D shallow water wave basin

Physical Model

To properly simulate real conditions, kinematically and dynamically, Froude scaling of 1 to 20 was chosen. Two physical models were used throughout the research, bridge model and flat plate model.

Bridge Model

One physical model was a 1:20 scale model bridge section. The model consisted of a deck, 6 girders, a sidewalk, and a guardrail made from acrylic. The model represents a 1:20 scale of a section of the U.S. 90 Bridge shown in Figure 1-1. The model remained at constant height of 0.48m from the basin floor measured from the bottom of the deck (0.41m from the bottom of the girders) which represents the elevation of the U.S. 90 bridge over the bottom away from the channel. Figure 3-2 shows a schematic of the model with dimensions. This model represented half of the prototype's (U.S. Highway

90 over Biloxi Bay) actual width, in essence, one concrete deck piece. Figure 3-3 shows a 3-D rendering of the prototype emphasizing the model representation.

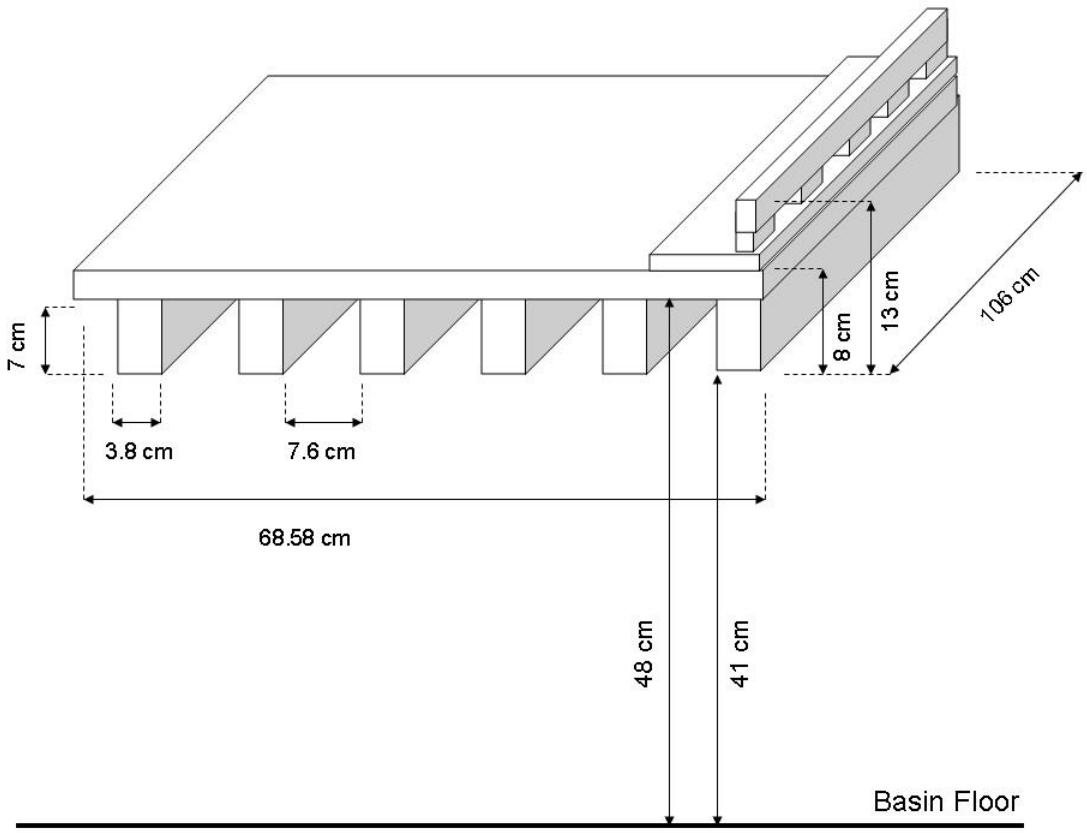

Figure 3- 2 Bridge model schematic with dimensions

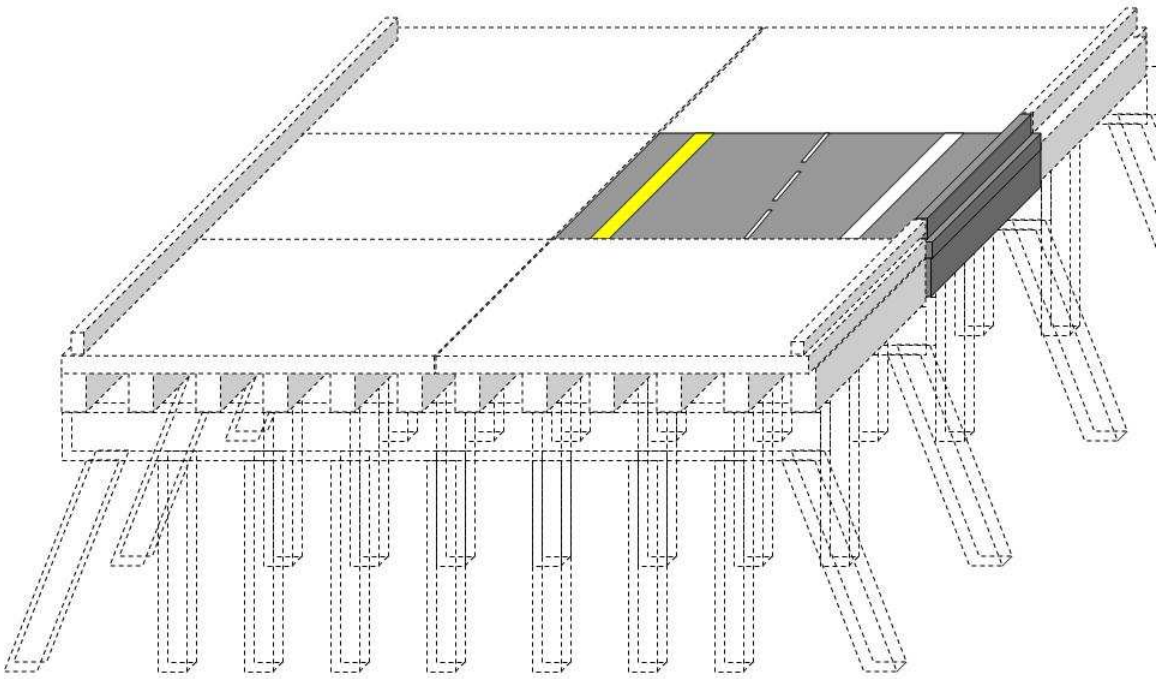

Figure 3- 3 3-D rendering of prototype section. Note the colored region is the portion tested by the physical model

Figure 3-4 shows the actual physical model during a test where a wave, traveling from right to left has inundated the specimen. Boundary effects present a significant problem with physical model test. In reality, the prototype bridge segment is continuous and spans across the bay. In order to take eliminate the boundary effects acrylic panels were placed on the sides of the model. The consequence of not having the acrylic panels would result in unrealistic 3 dimensional effects. These side panels can be seen in Figure 3-4. The acrylic sidewalls allowed for excellent underwater video during tests; however,

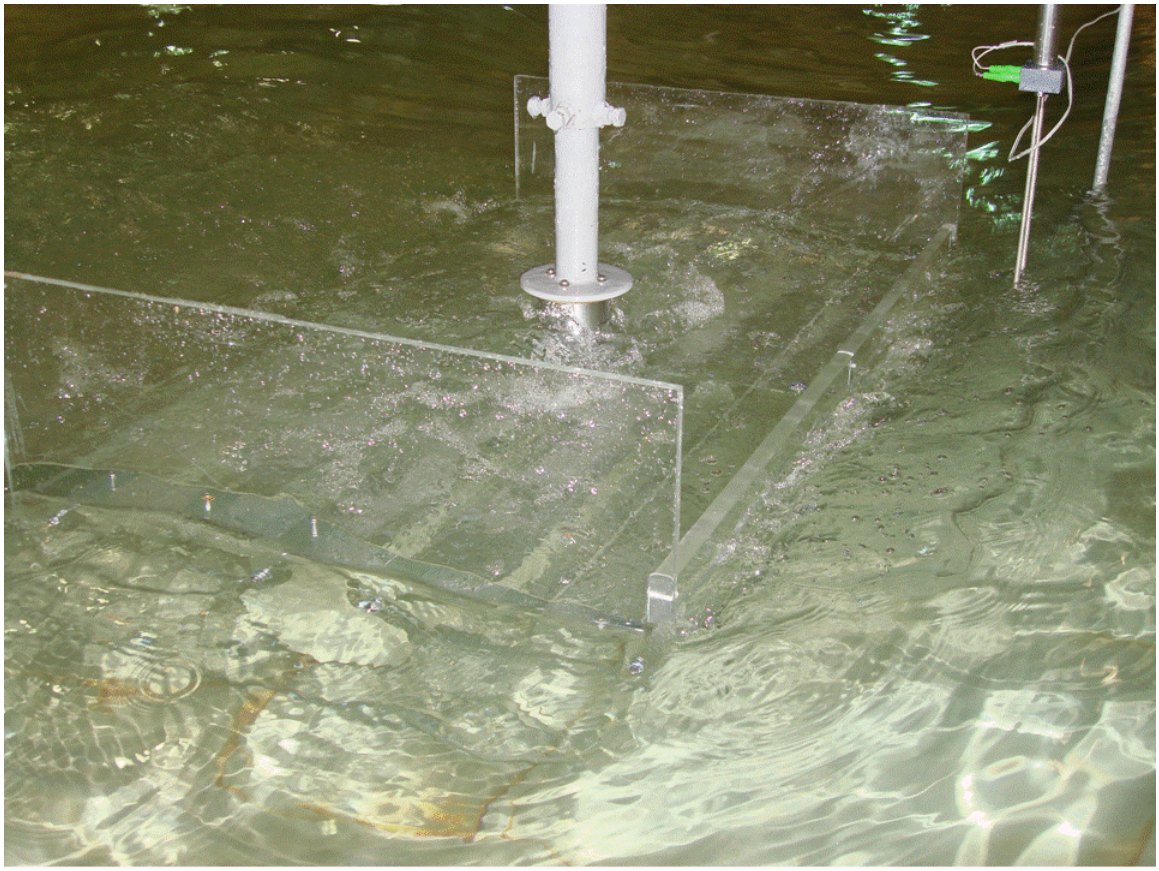

Figure 3- 4 Actual bridge model with acrylic side panels to account for boundary effects

its accuracy was questioned. Later in the research, dummy bridge sections were built and placed on both sides of the bridge model. This solution was speculated to be more accurate for two reasons. (1) The boundaries of the system were now pulled farther away than the physical model and (2) bridge pilings supported the dummy bridge sections creating a more realistic scenario. Figure 3-5 shows the two dummy bridge sections without the model bridge in between them.

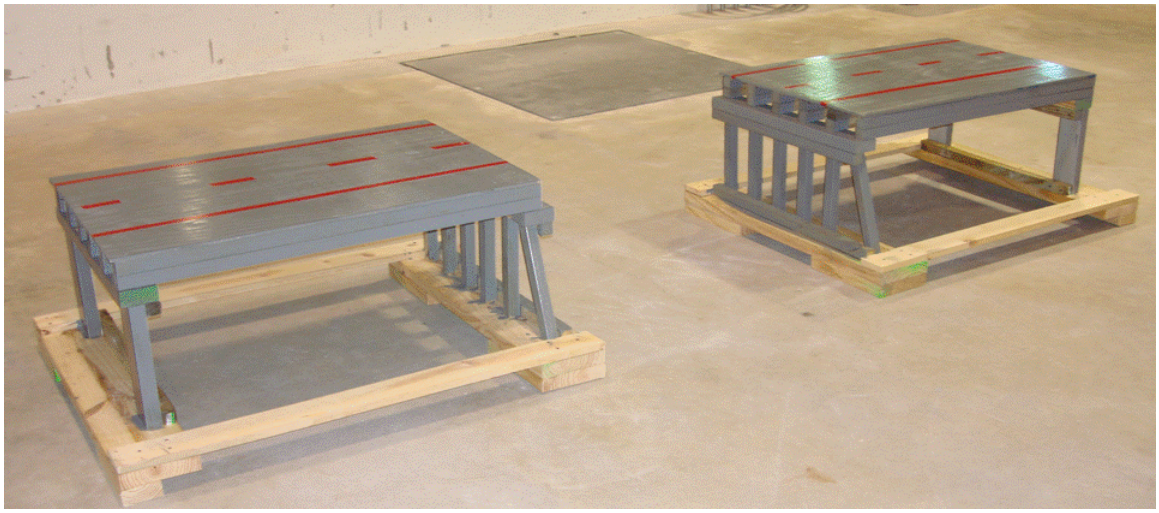

Figure 3- 5 Dummy bridge sections to account for boundary effects

Flat Plate Model

The second physical model used during the research was a simple flat plate. The dimensions of this physical model were identical in plan form to that of the bridge model (L: 1.06m W: 0.6858m). The model also remained at a constant height of 0.48m from the basin floor measured from the bottom of the plate. The original purpose of this physical model was to determine the force implications due to girders on a bridge deck. Moreover, the flat plate model provided the simplest geometry to evaluate uplift mechanisms. Boundary effects were also an issue with the flat plate model. Most previous theories are 2-dimensional with the assumption the structure is infinitely long. Therefore the same acrylic sidewalls used for the model bridge were used for the flat plate model. The schematic of the flat plate with sidewalls is shown in Figure 3-6.

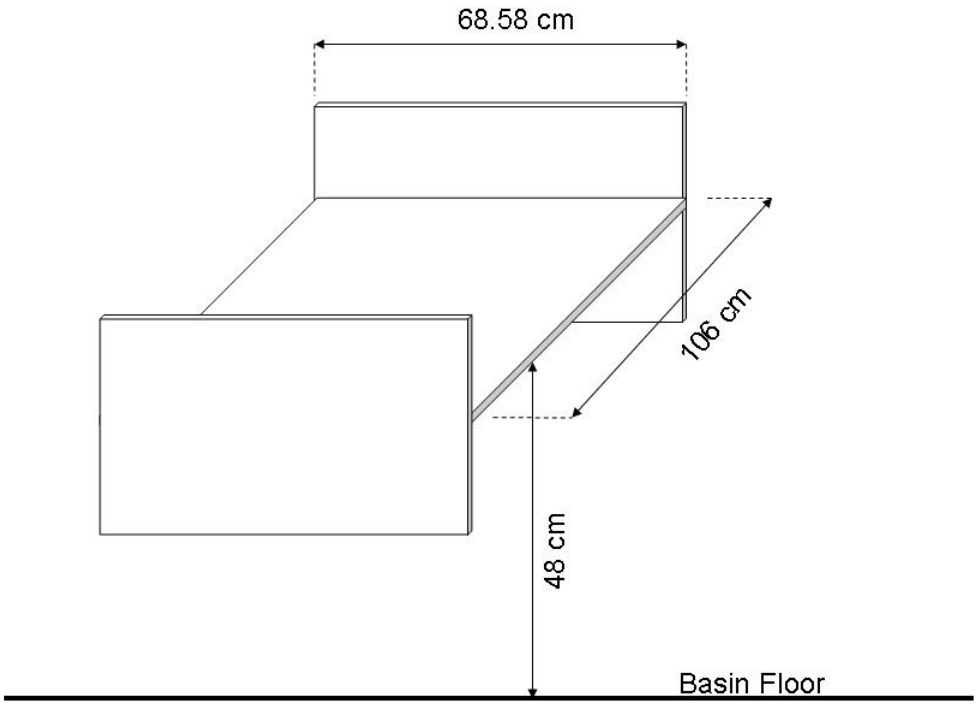

Figure 3- 6 Flat plate model schematic with dimensions

Testing Equipment

Several instruments were used to record information such as forces, waves, and visual data needed to complete the research. Other equipment was also needed to logistically accomplish the physical model experiments.

Logistical Equipment

The physical model was suspended from the top of the deck in order to make the experiment as non-intrusive as possible. To accomplish this, a catwalk bridge that spans the width of the basin was utilized. A large steel box apparatus was fabricated to hang securely (stiff) from the basin's bridge. The physical model was then attached to the box apparatus by a single cylindrical rod. The overall goal of the box apparatus was to

provide a stiff non-intrusive foundation to attach the physical model during testing. Figure 3-7 shows the box-apparatus (gray) attached to basin's catwalk bridge (blue).

Figure 3- 7 Hanging box apparatus attached to basin bridge

Force Measurements

The forces were measured from a single force transducer attached to the top center of the physical model. The force transducer separates the physical model from the stiff box apparatus. It delivers an analog signal with six degrees of freedom (F_x, F_y, F_z, M_x, M_y, and M_z) to an amplifier and then to a computer. The signal can be recorded at up to 200 Hz digitally or 1000 Hz analog.

Wave Measurements

Four resistance wave gages were used to measure the water surface at various locations in the basin at a sampling rate of 25 Hz. While the location of the gages differed between the test setups, there was typically a gage located well in front of the physical model, directly or closely in front of the physical model, and to the side of the physical model. The purpose of the side gage was to measure the water surface at the same distance from the wave generator as the physical model however unobstructed by the physical model itself. During some tests a wave gage was placed directly behind the physical model.

Visual Data

For some of the tests an underwater video camera was used. The camera was a simple USB video camera housed in a water proof capsule securely attached to the basin floor. The location of the camera varied to gain multiple perspectives. This provided valuable information for underwater and surface conditions during experimentation. Also used in some tests was a normal portable video camera. This was typically placed on the front side of the basin and provided a macro scale view as the physical model was inundated by waves.

Experimental Setup

As stated earlier, several sets of experiments were completed throughout the research. Each set was generally enhanced building off the last set in an effort to create

more accurate and informative tests. Items that varied throughout the research included physical model type, physical model placement, gage placement, boundary condition solution, and test procedure. The following outlines in detail the test setup for each set of experiments.

Experimental Set I

The main objective of this experiment was to test the bridge model at varying wave heights (H), periods (T), and water depths (h) for monochromatic waves. In all, 24 tests were run using wave periods of 1.3s, 1.8s, and 2.5s, wave heights of 0.10m, 0.12m, and 0.14m, and water depths of 0.41m, 0.48m, and 0.54. Each test consisted of 100 seconds of monochromatic waves. The physical model was moved to the rear-center of the wave basin. This allowed for a longer test time before the beginning waves corrupted the experiment due to the sequential reflection of the rock beach and wave generator. Of the four wave gages used, two gages were placed either side of the model equidistant from the wave generator. A third gage was set up approximately 0.1 m in front of the bridge specimen. The final gage was placed farther in front of the bridge model. Figure 3-8 shows a schematic of the basin for this experimental set. Acrylic sidewalls were attached to the bridge model to account for boundary effects.

Two underwater cameras were used during this round to record occurrences that were difficult to see while the tests were running. Several camera angles were tried throughout the testing period.

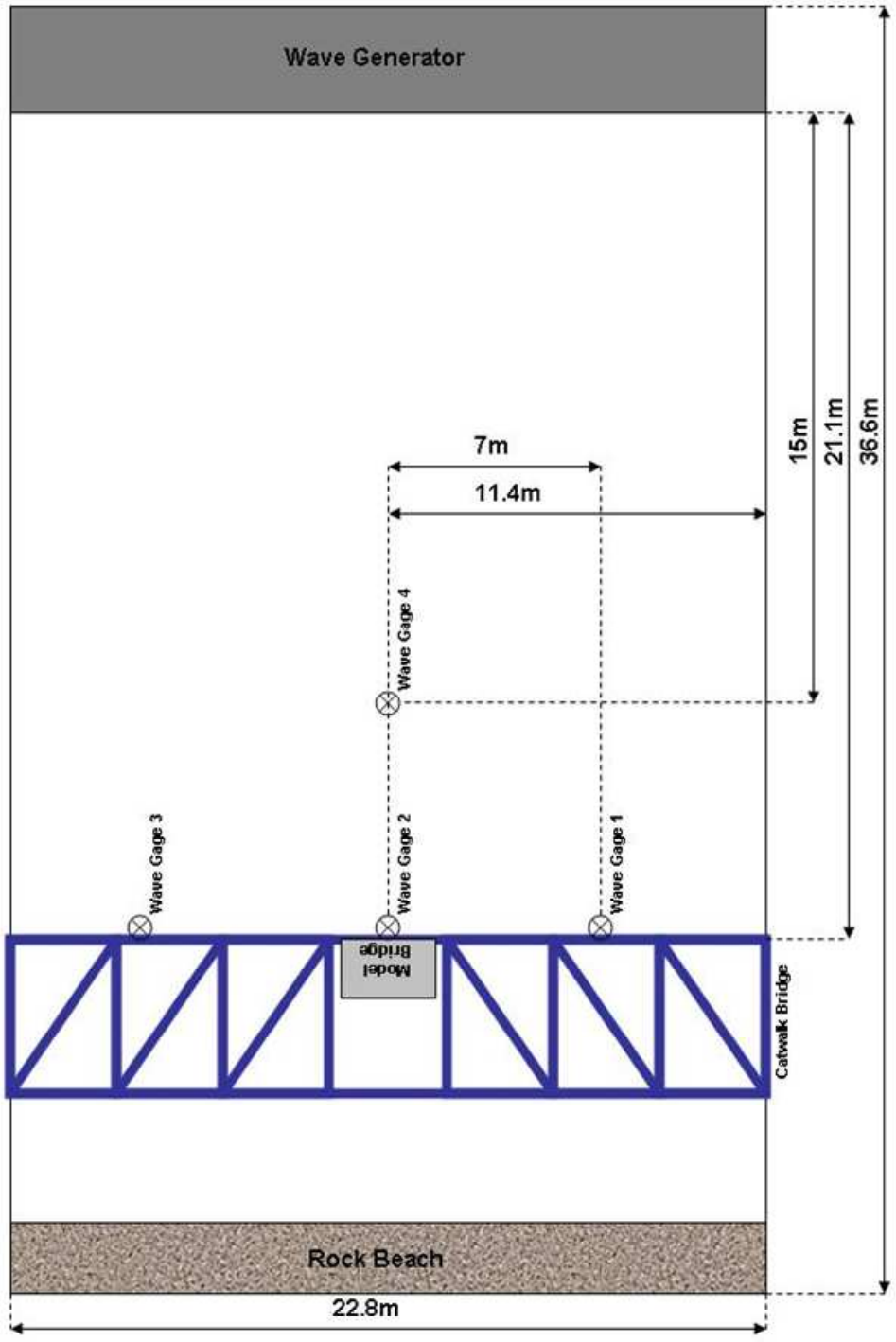

Figure 3- 8 Basin schematic for experimental set I

Experimental Set II

The main objective of this experiment was to test the flat plate model at varying wave heights, periods, and water depths for monochromatic waves. The physical model position, test procedure, and wave gage positions were identical to that of Experimental Set I. However, the test parameters varied slightly to investigate the effects of larger waves when the water depth had not fully inundated the structure. Thus, increased wave heights of 0.16m and 0.18m were tested for the water depth of 0.41m. In all 31 tests were run. Only one underwater camera was used during this set and filmed specifically the side view of the model as the waves passed. Unfortunately for this set, no side plates were installed on the flat plate and thus boundary effects were not taken into account. This consequently made the data from this experimental set difficult to work with.

Experimental Set III

The main objective of this experiment was to investigate in more detail the effects of varying water depth on the model bridge using monochromatic waves. During the analysis of the data from Experimental Sets I and II, an unexpected nonlinear trend in vertical force appeared when water depth alone was altered. Since the previous experiments only measured three water depths, this experiment was designed to investigate more increments of water depth. The wave height and period were kept constant at 0.14 m and 1.8 s respectively. In all 7 tests were run. The depths tested during Experimental Set III were 0.39m, 0.41m, 0.43m, 0.46m, 0.48m, 0.51m, and 0.54m. The same water depths 0.41 m, 0.48m, and 0.54m were tested to demonstrate

repeatability of the experiments. Again, each test consisted of 100 seconds of monochromatic waves.

The physical model was again located identically to that of Experimental Sets I and II. All of the wave gages except for the immediate front wave gage were set up identically to that of Experimental Sets I and II. The immediate front wave gage was now placed immediately in front of the bridge model instead of a distance 0.1 m.

The sampling rate of the force transducer was altered during this set to 1000 Hz. The previous tests were sampled at 200 Hz. The higher sampling rate was chosen to more accurately record the maximum force. Several previous literature state a short impact force accompanies the slow varying force. If the maximum force peak occurs in between samples, the true maximum force will not be recorded. The error of the smaller sampling rate depends on the sharpness of the force peak. It was found however, the difference in the maximum force peaks when recording at 200 Hz and 1000 Hz was indiscernible.

Experimental Set IV

The main objective of this experiment was to run the same tests as Experimental Set III with the flat plate model. Since the flat plate model is inherently thinner than the model bridge, the first water depth in which waves come into contact with the model is at 0.43m. Thus, the water depths tested were 0.43m, 0.46m, 0.48m, 0.51m, 0.54m. The wave height and period were again kept constant at 0.14 m and 1.8 s respectively.

The test setup and procedure, including the location of the model and gage placement was identical to that of Experimental Set III. However, the flat plate model for

this experiment had been drastically modified. Acrylic sidewalls were installed that were identical to the sidewalls on the model bridge to account for the boundary effects. It was also visually observed during Experimental Set II that the flat plate model undesirably flexed during wave inundation. This flexibility of the model absorbs a portion of the energy when a wave passes consequently producing inaccurate force measurements. Steel leading and trailing edges were attached to the flat plate to stiffen the overall model.

Experimental Set V

The main objective of this experiment was to test various water depths and wave heights on the bridge model using solitary waves. Experiments using monochromatic waves did not experience uniform waves or forces after the first half dozen waves because of wave diffraction from the incident waves coming into contact with the model and wave reflection off the sidewalls and rock beach. When a solitary wave is used there are no longer reflection and/or diffraction problems. On the down side, however, the sample size of the experiment is small compared to monochromatic wave tests. Each test consisted of a single wave.

Similar to Experimental Sets III and IV the smaller increments of water depth were tested and the period was kept constant. However, during Experimental Set V the wave height was altered using heights of 0.10m, 0.12m, 0.14, and 0.16m.

In order to more accurately represent the boundary affects the dummy bridge sections were implemented during this experimental set. As stated earlier the dummy bridge sections pushed the boundary effects farther away from the model bridge possibly making the test measurements more accurate. The dummy bridge sections also introduce

pile caps and pilings into the model which make the tests more realistic. Monochromatic waves were also run at each depth for comparison of boundary effect solutions.

The location of the bridge model was moved more towards the middle of the basin since each test consisted of only one wave and reflection was no longer an issue. The closer location of the model also allows the solitary waves to fully develop with minimal effects from the basin floor. Wave gage locations also differed. Only one gage was kept at the side of the bridge. One gage was placed well in front of the model and one gage was placed directly in front of the model. During this experiment set a wave gage was also placed directly behind the model.

Experimental Set VI

The main objective of this experiment was to investigate the effects of multidirectional waves on the model bridge using monochromatic waves. The test setup, including model position and dummy bridge sections was identical to that of Experimental Set V. The test procedure used monochromatic waves at varying angles of incidence. The water depth, wave height, and wave period were kept constant at 0.48 m, 0.14m, and 1.8 s respectively. In all there were 3 tests run. The angle of incidence tested was 0, 10, and 20 degrees. Figure 3-9 shows the model bridge in respect to the angle of incidence.

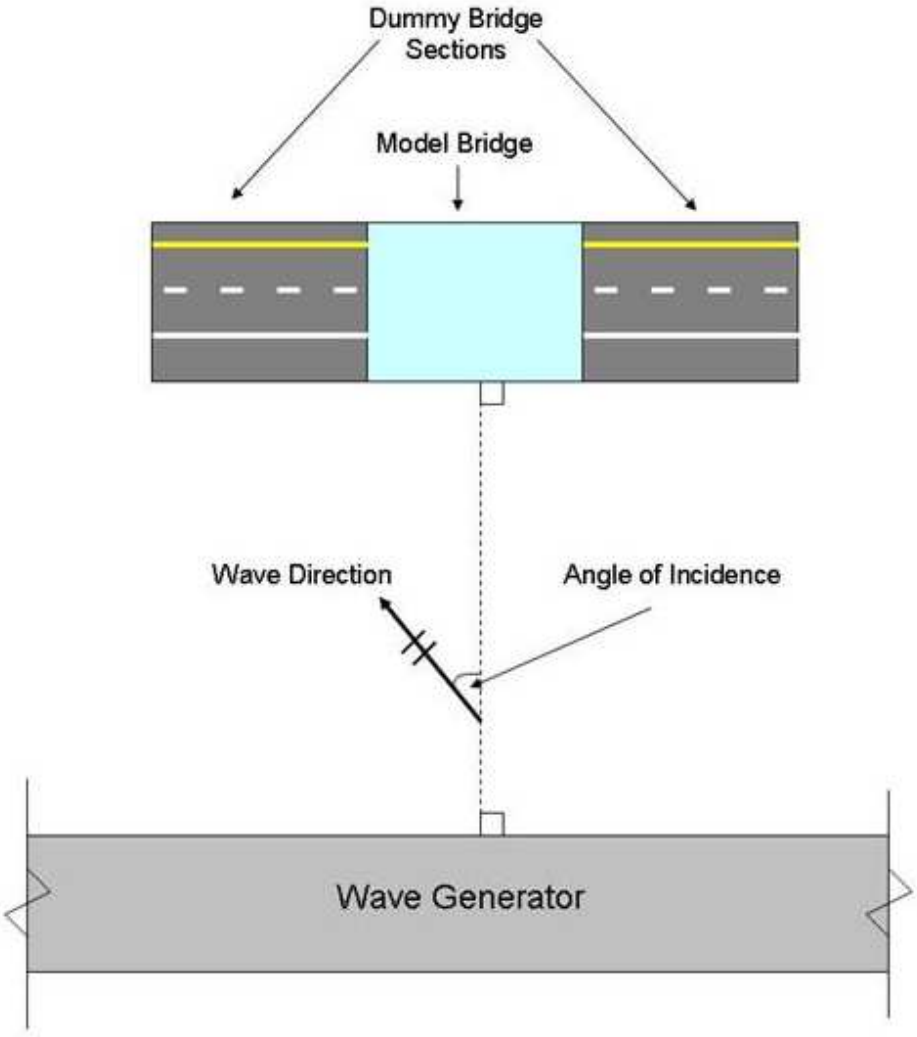

Figure 3- 9 Schematic of angle of incidence with respect to model bridge and wave generator

CHAPTER IV

DISCUSSION OF RESULTS

Three forms of data were recorded throughout the tests. Wave and force data were measured using resistance wave gages and a force transducer respectively. Visual data were recorded using video cameras. An underwater camera was used for some tests to observe occurrences underwater and at the water surface. A typical portable video camera was used for some tests to demonstrate the overall tests visually.

The goal of the research is to quantify forces on the physical models given a known wave condition. During the experiments using monochromatic waves, several waves inundated the physical model. The recorded wave and force measurements were synchronized. This provided the ability to match a forcing event with its corresponding wave event.

Waves

The water surface elevation was measured in the time domain. The raw data collected provided the water surface elevation with respect to the still water level, SWL versus time. While the waves created in these experiments could be intuitively identified visually, a technical wave event was identified using the zero up-crossing method.

Monochromatic waves in theory are perfectly uniform with each wave having identical wave conditions. In the laboratory the wave generator was designated a target wave condition. Once a wave was generated, it was then subject to the boundary effects of the floor and sidewalls of the basin. These boundary effects have a non-linear effect on the target wave by lengthening the trough and sharpening the crest. Because the water

depth is shallow, the waves generated during the research were not perfectly linear. Once reflection began and turbulent conditions were created at the bridge the wave were no longer identical. This however does not make the experiments invalid. To compensate for the variation, either each force event was identified with its corresponding specific wave condition instead of the target wave condition or the data were filtered to analyze only those force events associated with wave events that matched the target wave condition.

Forces

Forces acting on the bridge were recorded in three directions, x, y, and z. Since a majority of the tests were run with a zero degree angle of incidence the x component was ignored. Thus, the y and z components represented horizontal and vertical forces respectively. Due to the non-uniform nature of the waves, the force measurements were also not uniform for each wave event. It was found as expected after Experimental Set I that the vertical force experienced by the physical model was substantially greater than the horizontal force. Therefore the beginning of the research focused mostly on the uplift force.

General Trends

After completion of Experimental Sets I and II, the forces were analyzed by independently increasing the three parameters leaving the others constant. To more accurately analyze the data the wave measurements were filtered. The wave events that

best matched the target wave height were used with their corresponding force event. These force events were then averaged.

The effect of varying the wave period while keeping the water depth and wave height constant was reviewed. A general trend was found that the vertical force slightly increased as wave period increased. The change was not largely dramatic. Figure 4-1 shows a plot of typical increasing trend of vertical force as period increases.

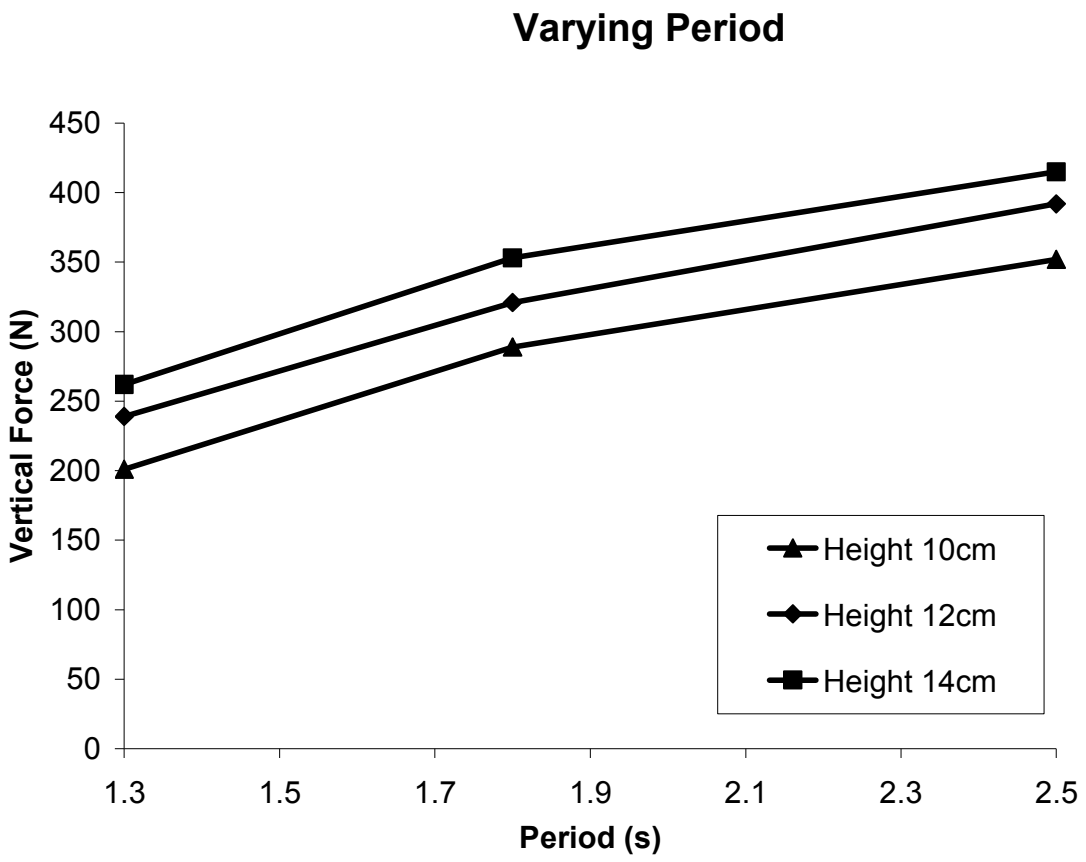

Figure 4- 1 Typical varying period

The effect of varying the wave height while keeping the water depth and wave period the same was also reviewed. A general trend was also found that the vertical force

increased as wave height increased. This trend was expected. Figure 4-2 shows a typical plot of the vertical force as the wave height increased.

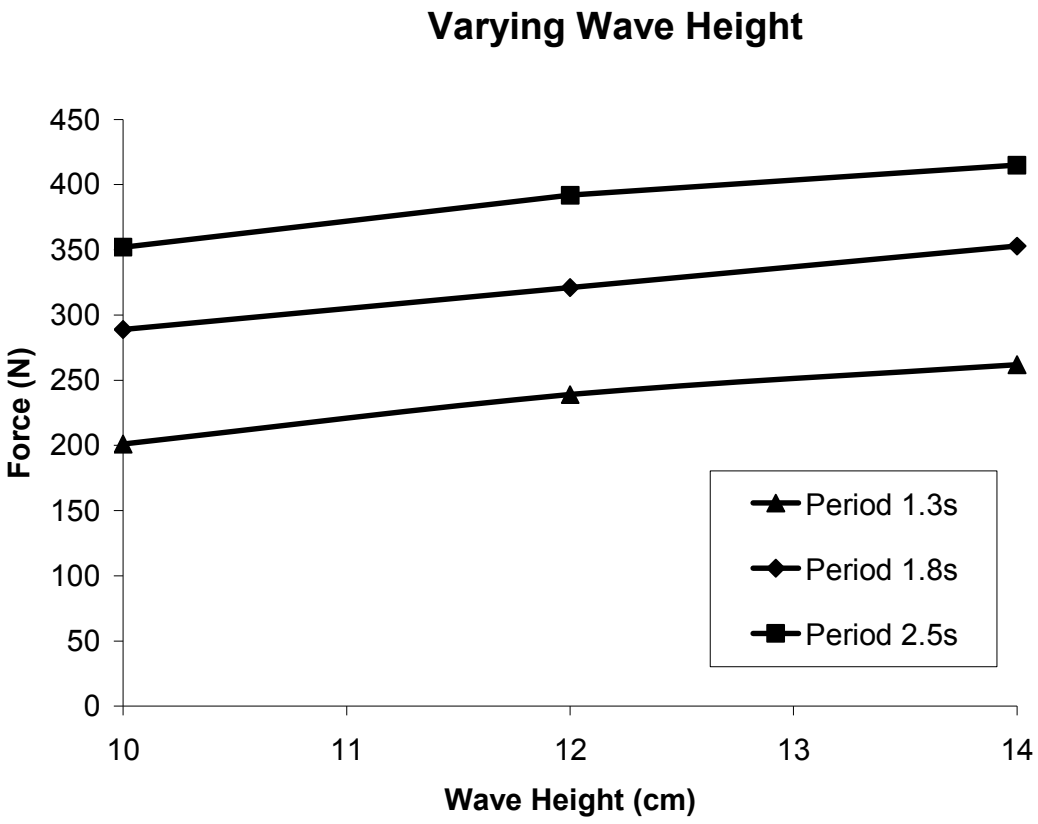

Figure 4- 2 Typical varying wave height

The effect of varying the water depth while keeping the wave height and period constant produced a substantially non-linear trend. Experimental Set III and IV more closely investigated this observation to better represent the trend. Figure 4-3 shows this trend for the model bridge and flat plate when the wave height and period had been kept constant at 0.14m and 1.8s respectively. An important note about Figure 4-3 is the buoyancy of the structures under the SWL has been removed (zeroed-out). The forces seen in the figure are caused solely by the wave. Both the model bridge and flat plate

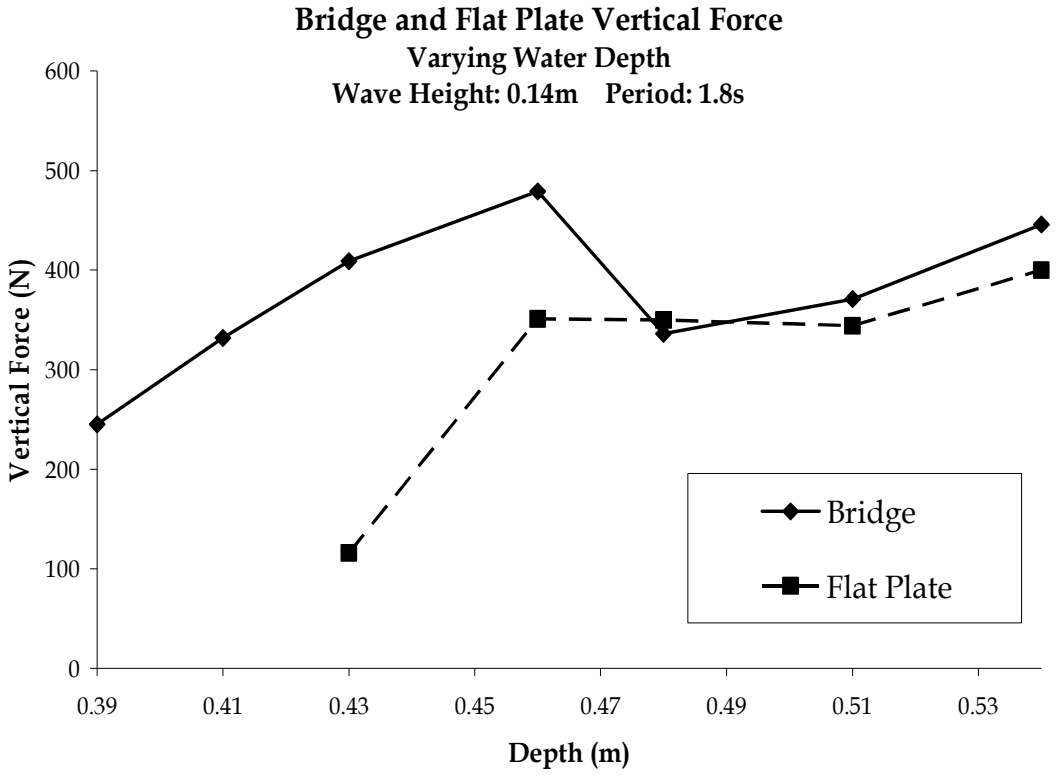

Figure 4- 3 Varying depth bridge and flat plate vertical force

showed similar non-linear trends, however the model bridge is more dramatic. It can be observed that the forces from the models converge at a depth of 0.48m. At this depth the SWL is at the base of the deck level for both models. At higher depths the uplift forces deviate very little.

Force Profile

Since the reason for this non-linear trend was not fully understood, the forces were then investigated in more detail by analyzing the force time series. Figures 4-4 and 4-5 shows the progression of the flat plate model force profiles as the water depth

increases. The flat plate model was chosen for the detailed analysis because of its simple geometry. When the SWL is significantly lower than the specimen (depth of 0.43m)

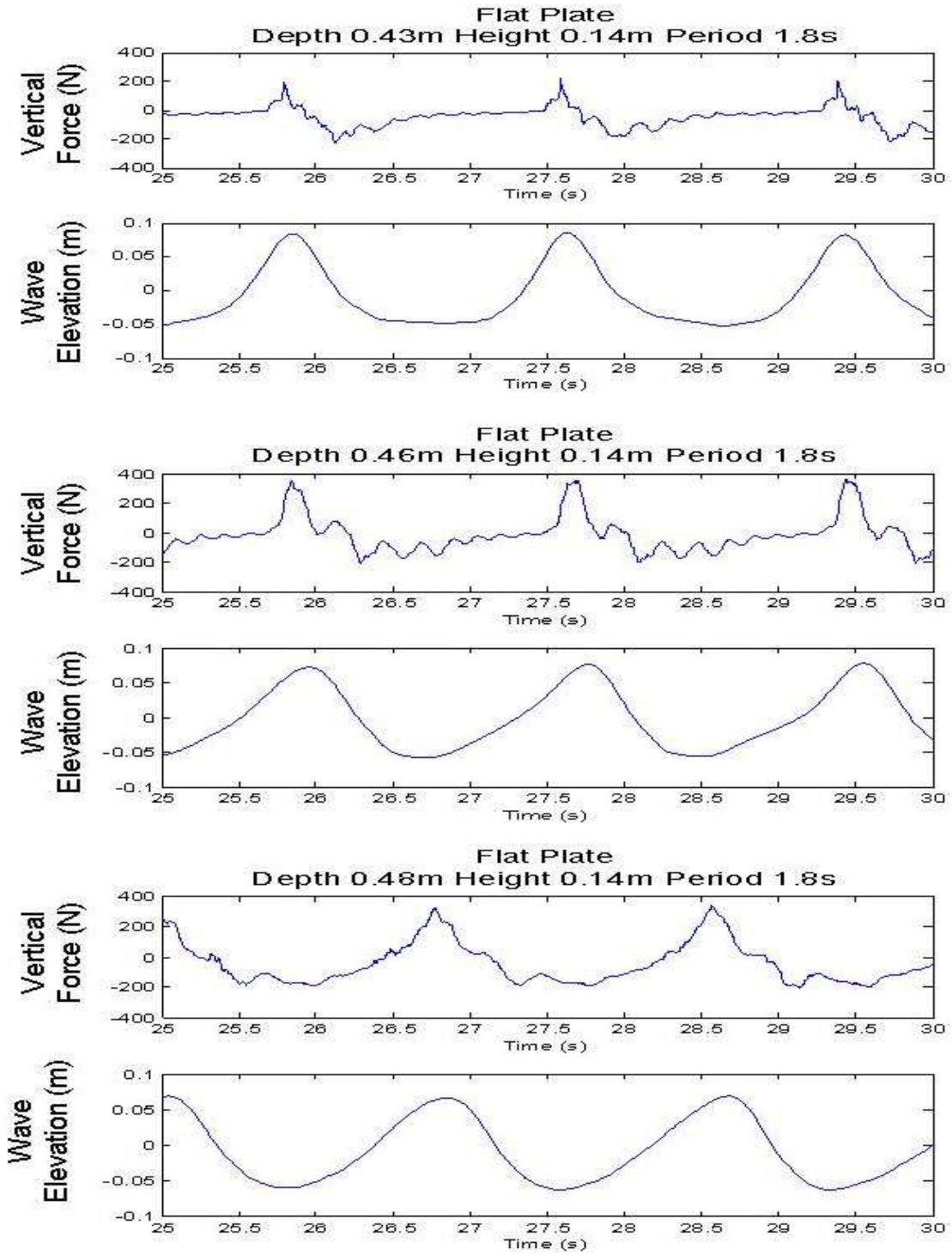

Figure 4- 4 Force progression as water depth increases (1 of 2)

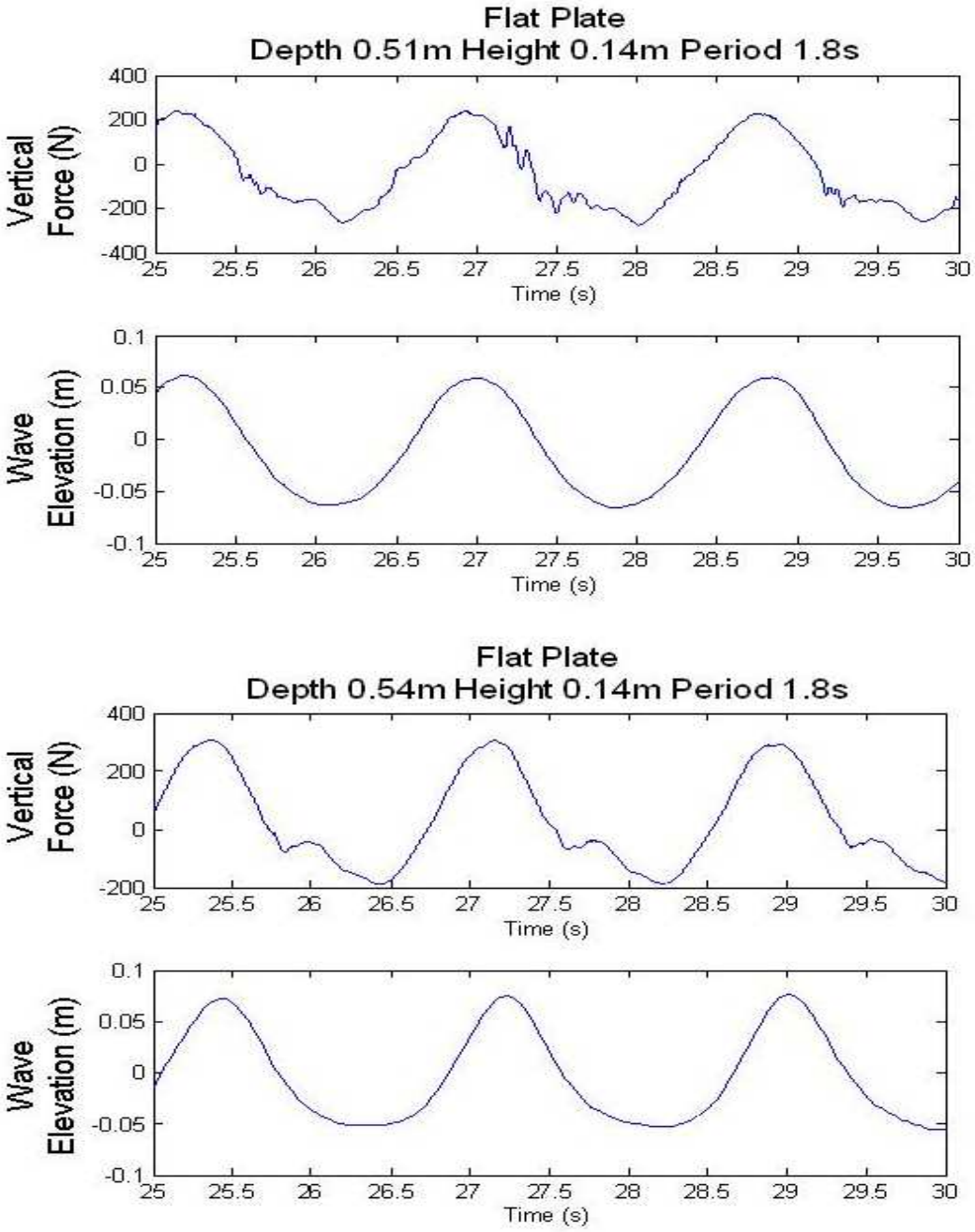

Figure 4- 5 Force progression as water depth increases (2 of 2)

this allows only a small portion of the wave to hit the model. The result is a short duration impact. As the depth increases the impact load is lessened. Eventually the depth reaches to a point where the model is fully submersed (Depths 0.51m and 0.54m)

and the force profile simulates an oscillating curve with a corresponding frequency of the wave's natural period.

An important observation from these plots is the location of the wave crest to the maximum force. The wave data shown in these figures is the wave train taken from the Gage 1 (refer to Figure 3-8). Recall the position of Gage 1 is equidistant with the leading edge of the physical model from the wave generator but unobstructed by the physical model. This represents the water surface that would exist if there had been no structure in the water. For the most part, the maximum force occurs at or just before the wave crest. In spatial terms, this means the maximum force occurs when the wave crest reaches the leading edge of the specimen (if the specimen were a bridge, the leading edge would be where the guard rails are). This observation suggests that the dominant uplift forcing on the model is hydrostatic. The maximum hydrostatic force for any object occurs when there is the largest height difference in water levels. This occurs for the model when the largest height above the deck level (wave crest) reaches the leading edge. In contrast, the maximum hydrodynamic force occurs closer to the center of the model which is explained in more detail in the next chapter.

Solitary Wave Results

The purpose of the solitary wave experiment was to gather more discernable data than that of the monochromatic experiments. As discussed earlier, after the first few waves passed the structure the wave train became non-uniform. Since the solitary wave tests consisted of a single wave event, contamination of the waves due to basin boundary effects was no longer a concern.

An item of extreme interest from the experiment was the location of the wave during the maximum vertical force. It was observed again that the location of the wave during the maximum vertical force was a short time before the crest reached the front of the structure. It was also now clearly observed that the location of the maximum horizontal force changed in reference to location of the maximum vertical force over the water depth. At lower water depths the location of the maximum horizontal force was aligned with the locations of the maximum vertical force. As the water depth fully inundated the model the maximum horizontal force was then delayed slightly (out of phase) with the vertical force. This suggests a possible hydrodynamic influence as the model becomes further submerged. Figures 4-6, 4-7, 4-8, and 4-9 show vertical and horizontal force profiles aligned with wave profiles taken well in front of the bridge, immediately in front of the bridge, and immediately behind the bridge over varying water depth. The bridge model is superimposed into the figures to provide a height reference for the waves as they impact the bridge model. The high frequency vibrations seen in the force plots, especially the horizontal force, are the natural vibrations of the structure.

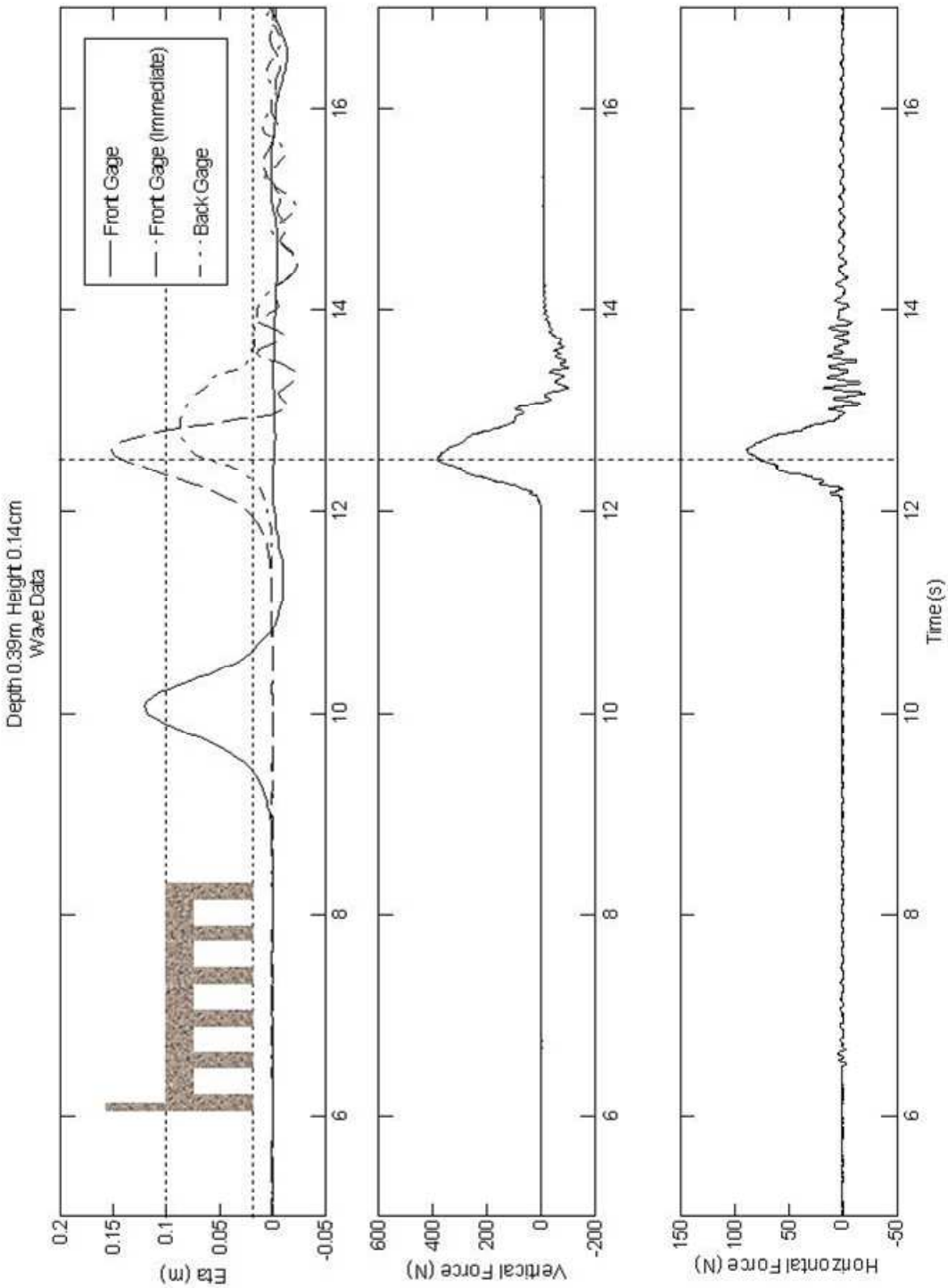

Figure 4- 6 Solitary wave and force time history at 0.39 m depth

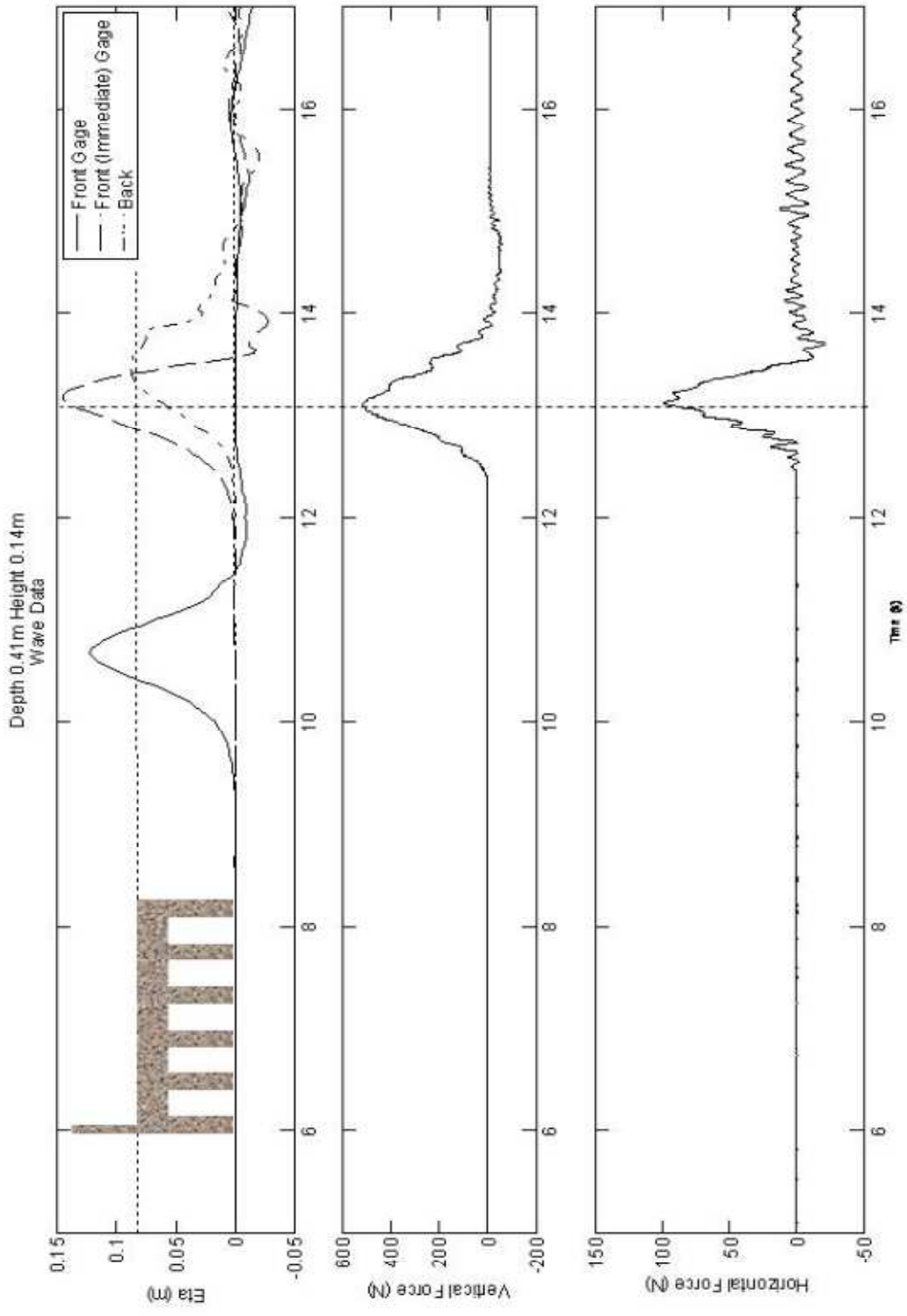

Figure 4- 7 Solitary wave and force time history at 0.41 m depth

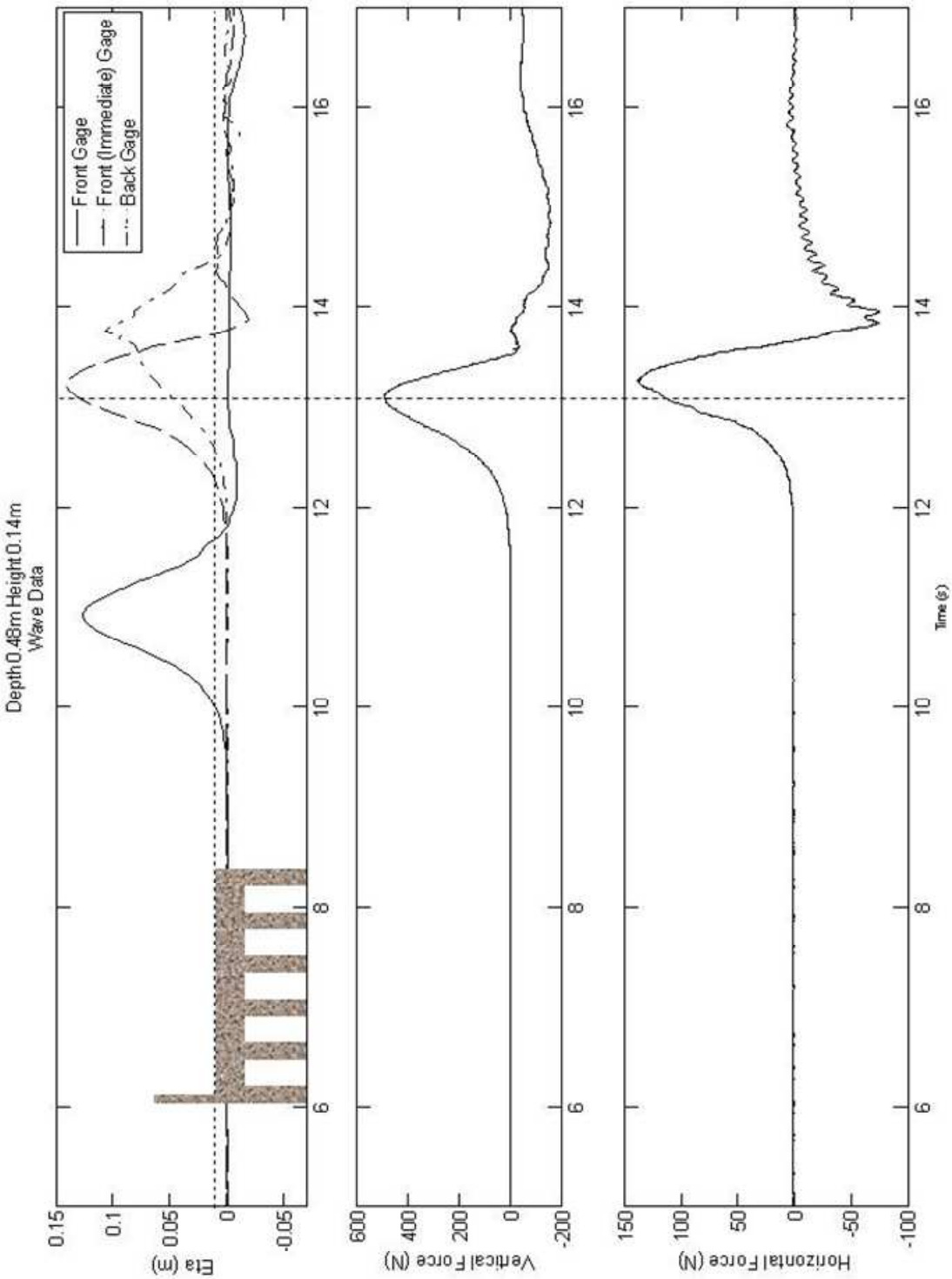

Figure 4- 8 Solitary wave and force time history at 0.48m depth

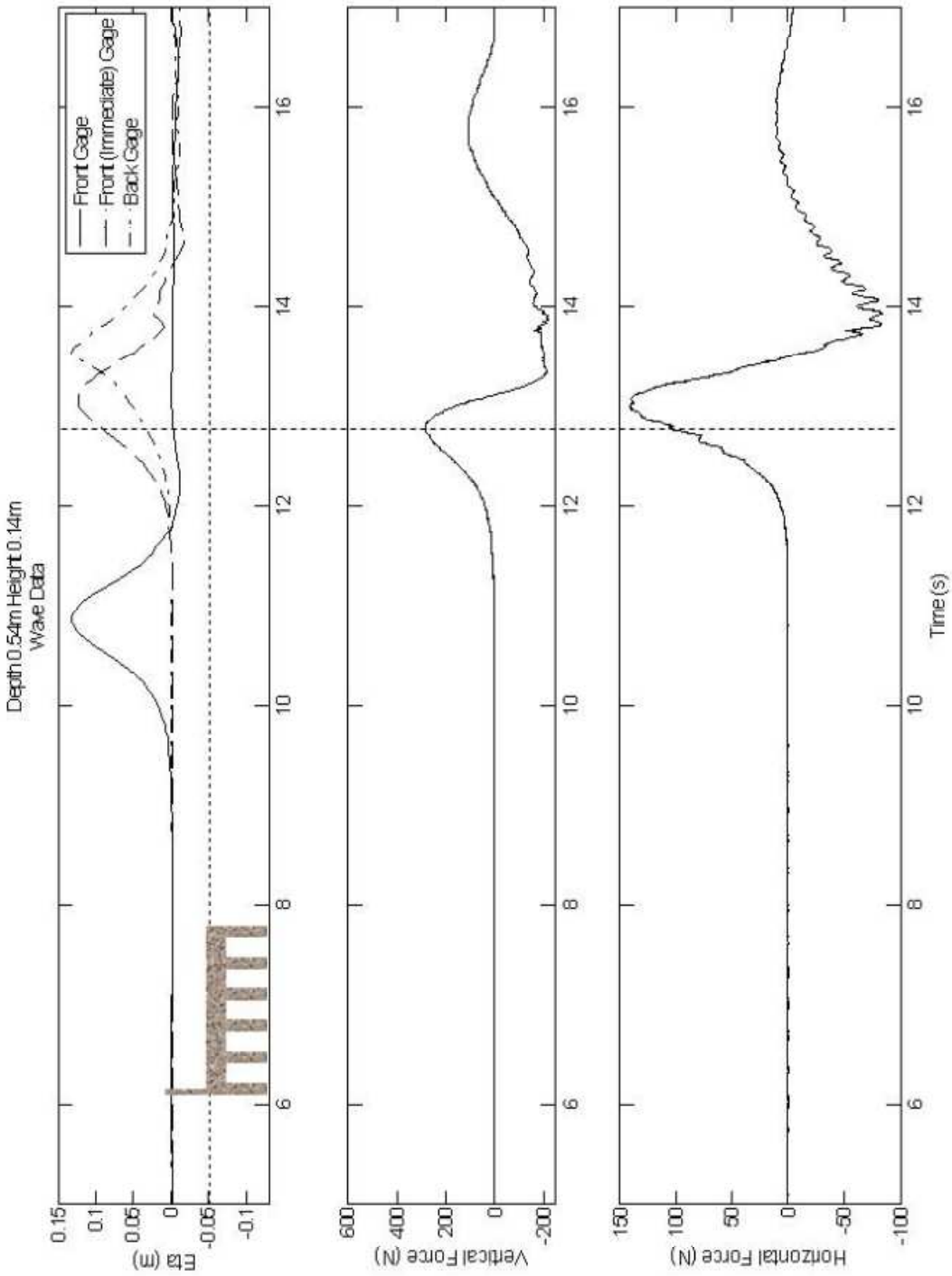

Figure 4- 9 Solitary wave and force time history at 0.54 m depth

As stated earlier, when force trends were investigated using the monochromatic experiments, the data needed to be filtered to provide forces that corresponded to the waves that best fit the target wave condition. Once again since the solitary wave is a single event, filtering was not needed. This provided a more discernable force trend over varying depth. Figure 4-10 and 4-11 show how the vertical force and horizontal force vary over water depth, respectively. The forces are plotted with respect to the water

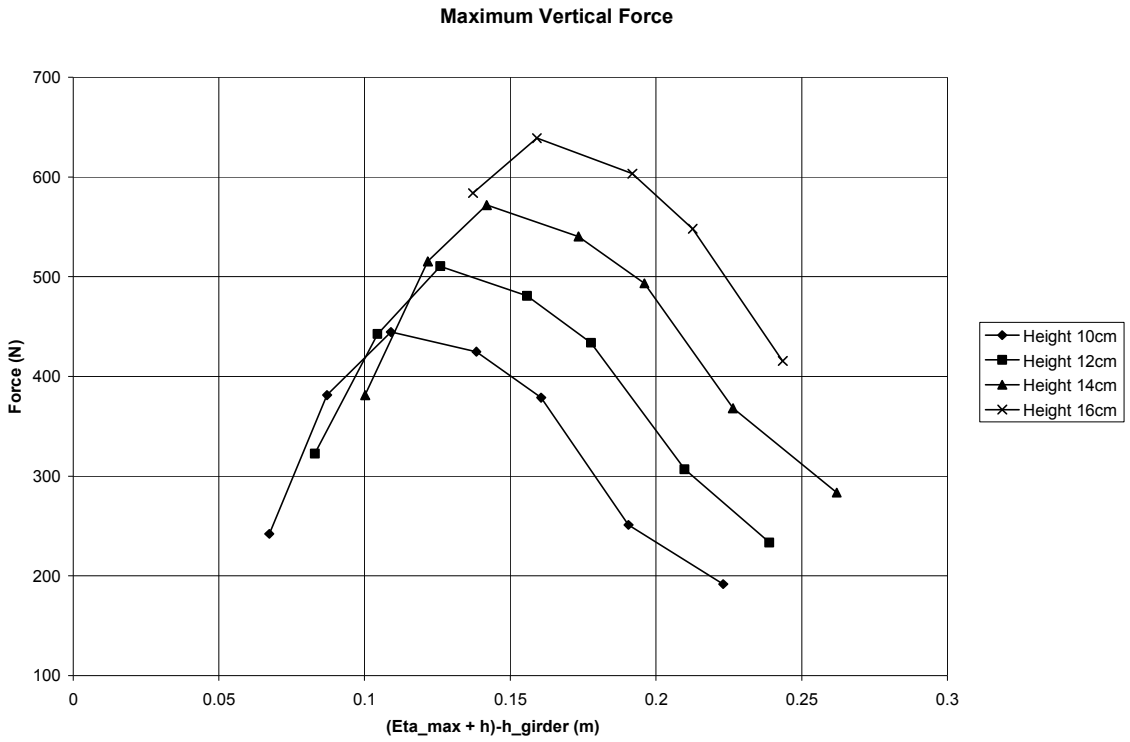

Figure 4- 10 Vertical force compared to water surface height above model

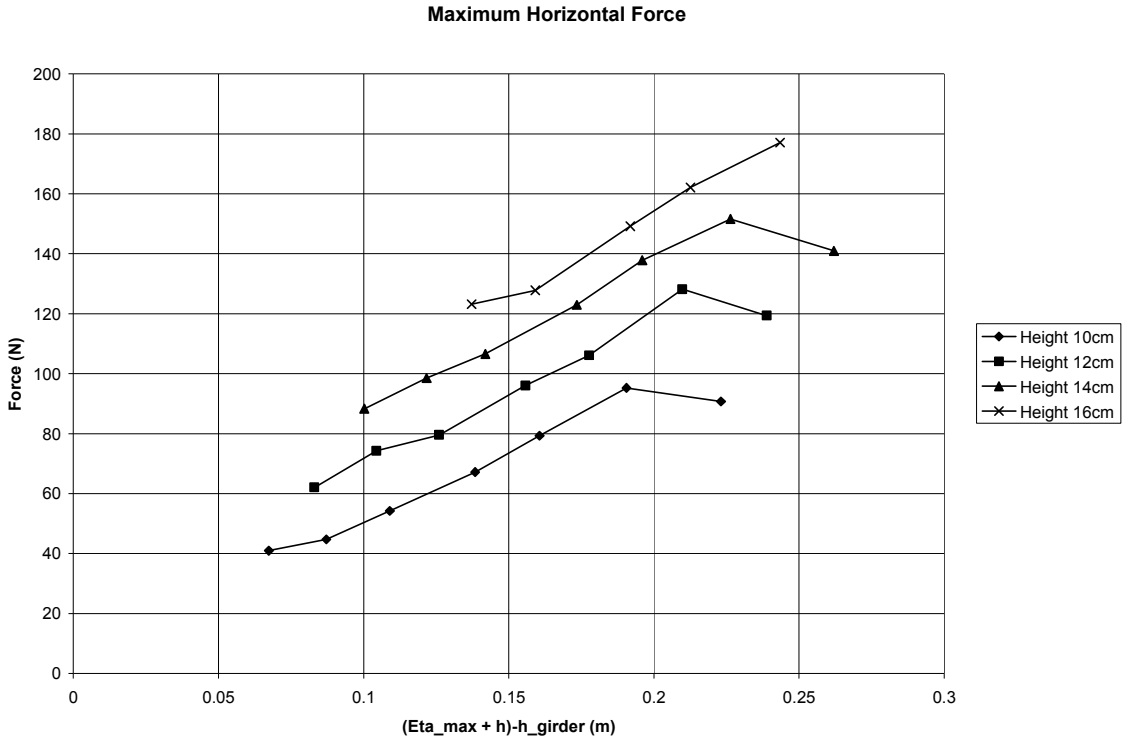

Figure 4- 11 Horizontal Force compared to water surface height above model

surface measured from the basin floor. Each point represents an individual solitary wave tests. The dominant parameter in hydrostatic forcing is the difference in overall water surface height and the structure. Therefore these plots will show a hydrostatic trend if it is present. Indeed a clear trend is seen in both vertical and horizontal force plots. The vertical forces rise, peak, and subsequently fall. The rise associated with each water depth seems to follow the same linear path. Each water depth then peaks at different level and falls. The horizontal force rises linearly and seems to level out at a certain point. Since neither plot show a conveniently straight line correlation, it can be concluded that vertical and horizontal force are not a simple function of maximum water height. Instead, there must be other factors or parameters involved. The suggested method for force estimation discussed in Chapter VI presents a theory of possible factors.

Air Entrapment

Post-storm investigations of coastal bridge failures often speculate about uplift force due to air entrapment between the bridge girders. The consequences of air-entrapment to coastal bridges could be devastating. If 100% of the air was trapped between the girders during a surge event, this could create a buoyancy force on the same order of the actual weight of the bridge. Understanding the presence or absence of air-entrapment is a large contribution to the overall uplift force produced during a storm event.

To investigate if air-entrapment actually occurs, underwater cameras were placed on the side of the model bridge. After tests were run, air-entrapment was indeed observed for water depths below the deck height. During the tests in which acrylic panels were attached to the model bridge a clear view of the space between the girders could be recorded. As a wave inundated the bridge, water was unable to completely fill in the space between the girders. The amount of air trapped between the girders was observed to change with every wave event. However, it was never observed that 100% of the air was trapped between girders.

CHAPTER V

COMPARISON OF PREVIOUS METHODOLOGIES

Previous literature offering force prediction methodologies were compared to measured horizontal and vertical forces from the various experiments. The literature used for the comparison was Bea et al. (2001), Kaplan et al. (1995), McConnell et al. (2004), and Douglass et al. (2006). As stated in Chapter II, the Kaplan and Bea methods are based on the equations from Morrison (1950). The forces prediction for these methods is purely hydrodynamic. This means the accelerations and velocities of the fluid provide the dominant forcing on the physical model. The McConnell and Douglass methods are purely hydrostatic. This means the dominant factor in the force prediction is the height of the water surface compared to the physical model.

Bea

As previously stated, Bea (2001) does not explicitly describe vertical force on decks. However, the method described for horizontal forces can be used to determine vertical forces by changing the horizontal components of velocity and acceleration to the vertical components. Linear wave theory states that the water particle velocity and acceleration are sinusoidal and 90^{o} out of phase. Therefore to accurately represent the force on a structure, the force components needed to be superimposed over an entire wave length. Recall that the vertical force components equations of the total vertical force are as follows.

$$Fs = 0.5\rho C_s Au^2 \quad (5\text{-}1)$$

$$Fl = 0.5\rho C_l Au^2 \quad (5\text{-}2)$$

$$Fi = \rho C_m Va \quad (5\text{-}3)$$

$$Fb = \rho gV \quad (5\text{-}4)$$

Where F_s, F_l, F_i, and F_b are the slamming force, lift force (vertical drag), inertial force, and buoyancy force respectively. The recommended values of the lift, inertial, and slamming coefficients used were 2, 2, and 1.5π respectively. The following figure is a typical flat plate vertical force profile using the Bea method separated into force components and total force.

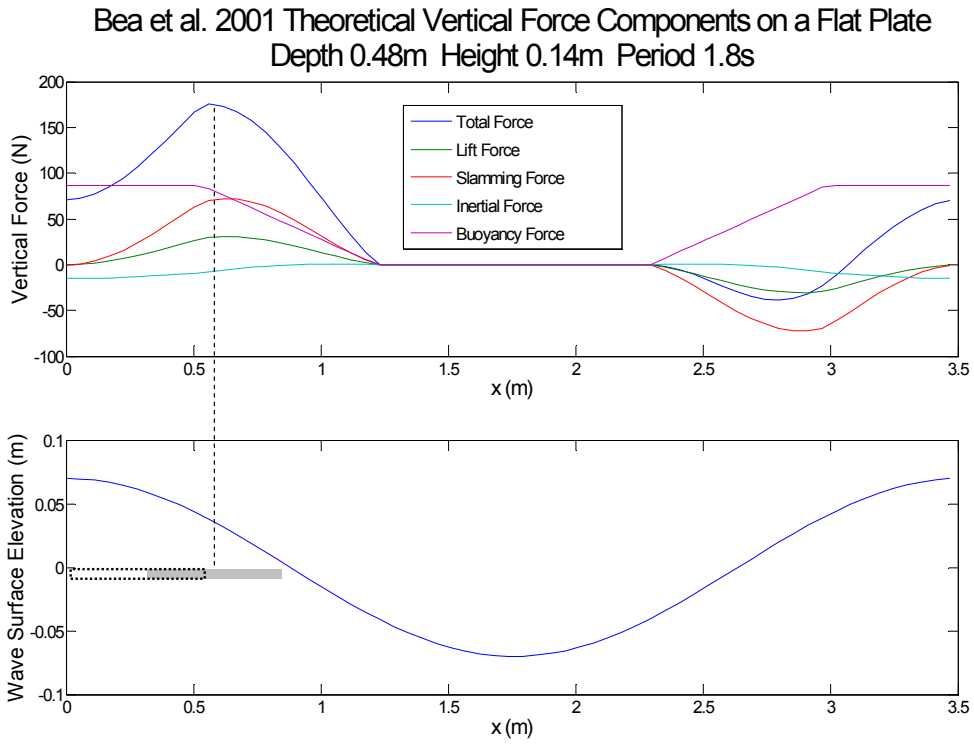

Figure 5- 1 Bea et al. 2001vertical force over a wave length

According to the Bea method, the location of the flat plate relative to the water surface during the maximum vertical force is shown in Figure 5-1 by the gray box. It can be seen that the location of the flat plate during the maximum vertical force in the experiments happens just before or right when the crest arrives at the leading edge of the structure. This is shown in Figure 5-1 by the dotted box. These locations of maximum vertical force are not in congruence.

It can also be observed in Figure 5-1 all of the force components go to zero for some duration. This is due to the wetted surface area going to zero. As the wave trough passes the structure, according to linear theory, no water will be in contact with the structure and therefore the force is zero.

Kaplan

The Kaplan et al. (1995) method is very similar to the Bea et al. (2001) method except there is no slamming component and the vertical inertial force, F_i is found using the 3-dimensional added mass of the structure. Once again the total force needs to be calculated by superimposing the force components over an entire wave length. Recall that the condensed vertical force equation for Kaplan et al. (1995) is as follows.

$$F_z = \frac{\partial}{\partial t}(M_3 w) + \frac{\rho}{2} b l C_D w|w| \qquad (5\text{-}5)$$

Figure 5-2 shows the vertical force components and the total force over an entire wave length for a flat plate at a distance 0.48m from the floor with a wave condition of H=0.14m, T= 1.8s, and h=0.48m. A drag coefficient of 2 was used to determine the lifting force component. The maximum force occurs at about halfway between the crest

and the trough. This location of the maximum force is not congruent with the experimental data.

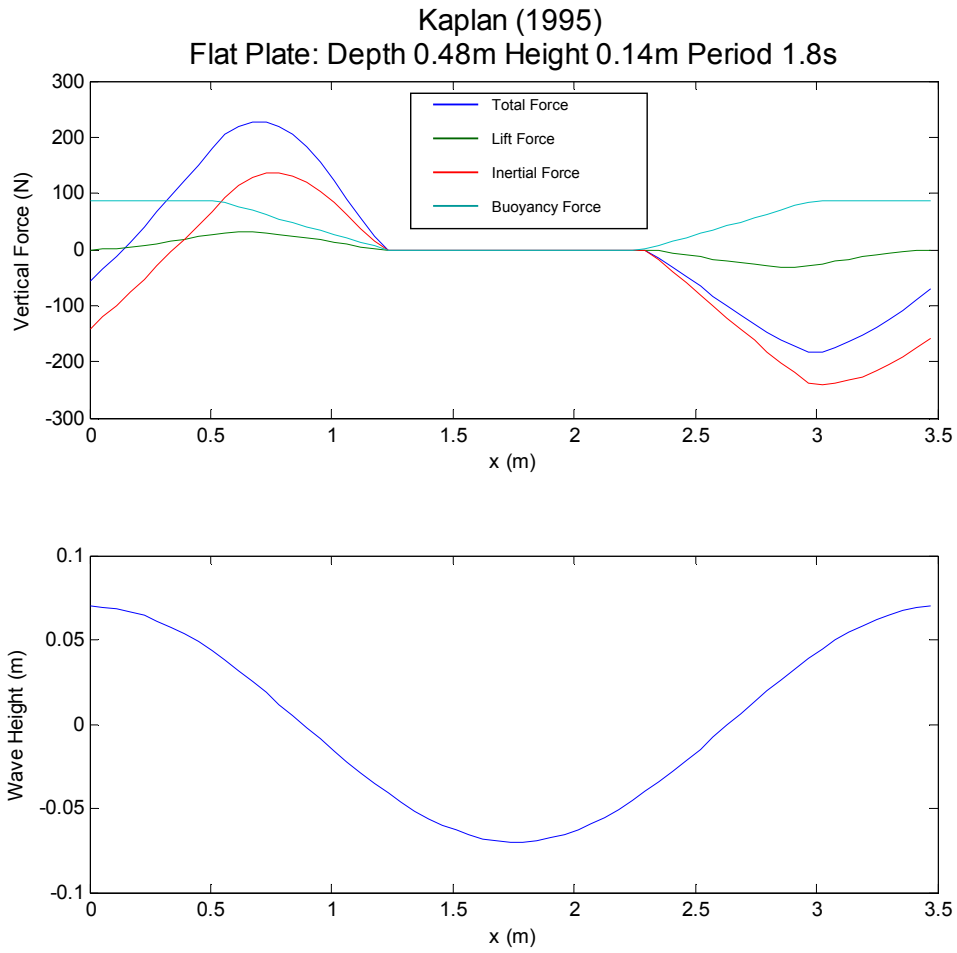

Figure 5- 2 Kaplan et al. 1995 vertical force over a wave length

It was observed from the bridge specimen that as the period of the wave increased keeping the wave height and water depth constant the vertical force increased. Figure 5-3 shows how the Kaplan method predicts the vertical force as the period is varied keeping the water depth and wave height constant.

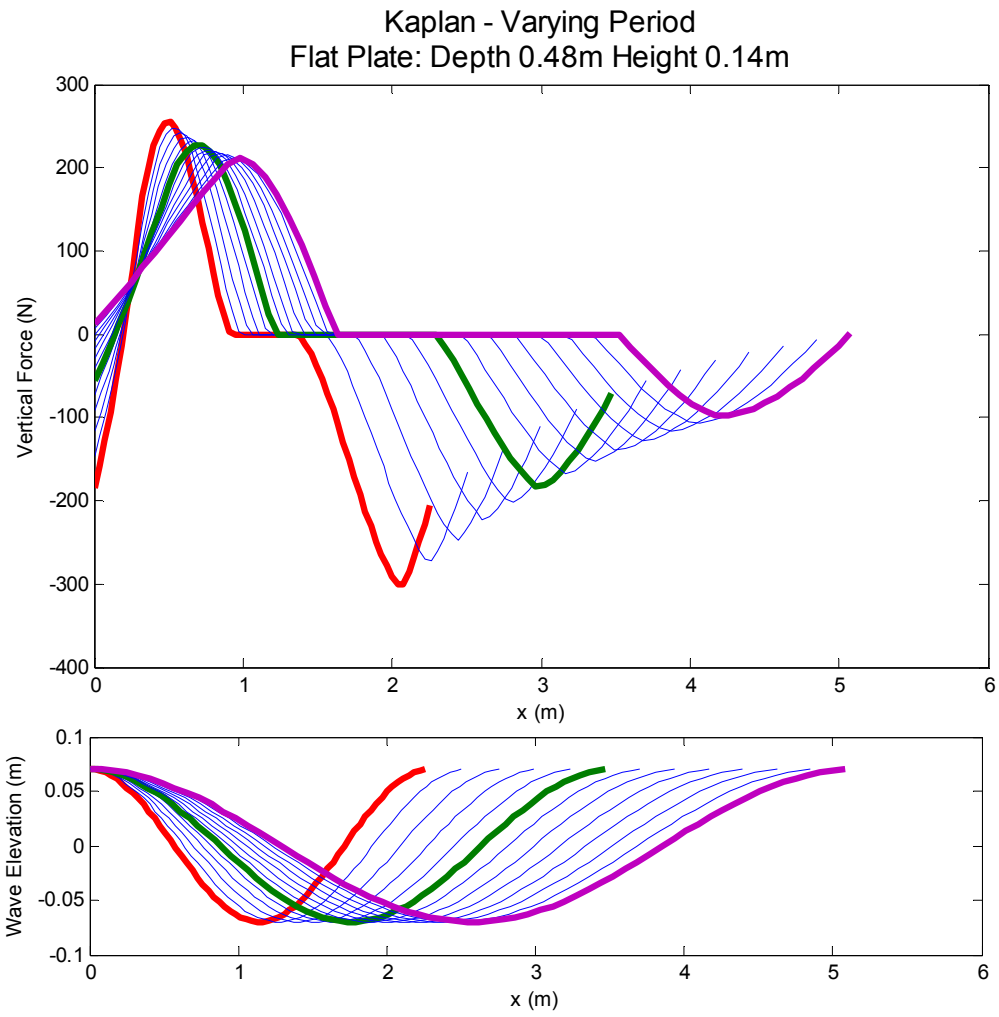

Figure 5- 3 Kaplan et al. 1995 vertical force varying period trend

The red, green, and purple lines represent the 1.3s, 1.8s, and 2.5s period waves respectively. As the wave period increases the maximum vertical force begins to decrease nonlinearly. This is opposite of what was observed during experimentation.

McConnell and Douglass

The McConnell and Douglass methods are hydrostatic and do not require analyzing over a wave length. The main factor in force prediction for these methods is the height between the wave crest elevation and the structure. Both methods are

empirical. The recommended empirical coefficients from the literature were used for the comparison of the methods to experimental data.

Correlation of Previous Methods and Measured Forces

Numerous waves and consequently force events were generated and recorded over all the experiments. This data were accumulated and made into comparison plots to visually and quantitatively show the comparison of previous methodologies to measured forces. The data from each wave event was used to calculate an estimated force for each method and then compared to the corresponding force recorded from that wave event.

Since the Bea and Kaplan methods are based on wave height, period, and water depth each wave event had to be individually processed. The period and water depth used for the Kaplan and Bea calculations was the target wave period and basin water depth. The wave height was determined using the zero up-crossing method where the wave height was calculated by subtracting the wave crest elevation from the wave trough elevation of the determined wave event. The McConnell and Douglass methods used only the wave crest elevation from each wave event to calculate the estimated force.

Monochromatic Waves

Figures 5-4 – 5-7 show each of the previous methods compared to the actual measured vertical forces on the flat plate using monochromatic waves. The data for Figures 5-4 – 5-7 were collected during Experimental Set IV

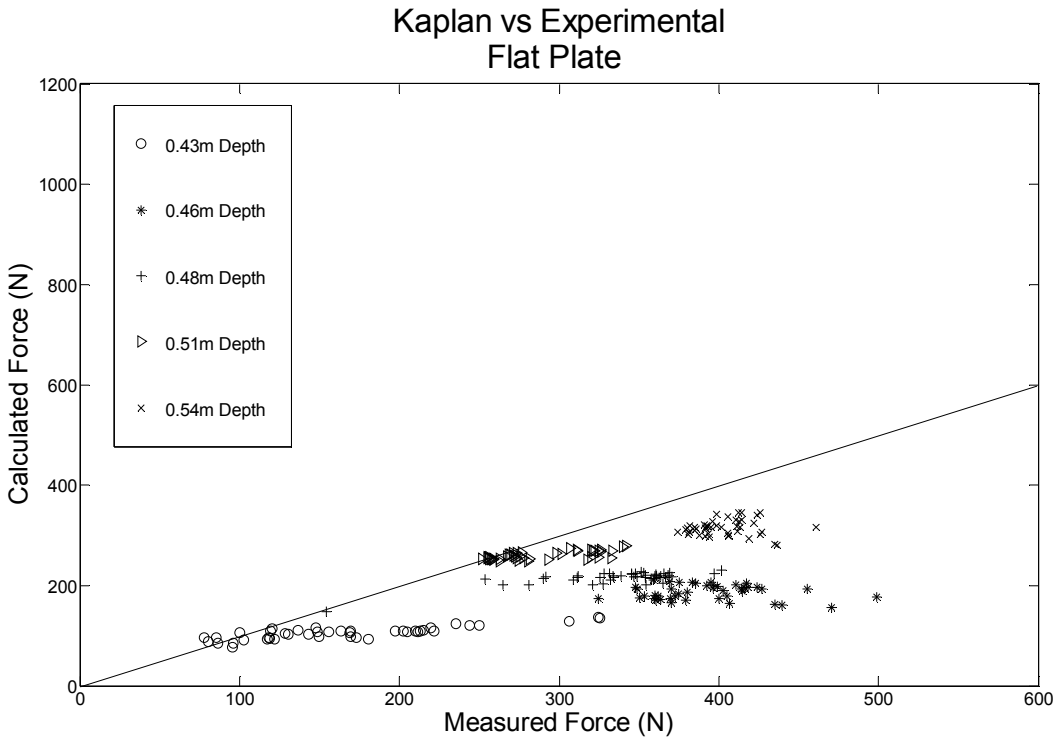

Figure 5- 4 Kaplan method compared to vertical force measurements

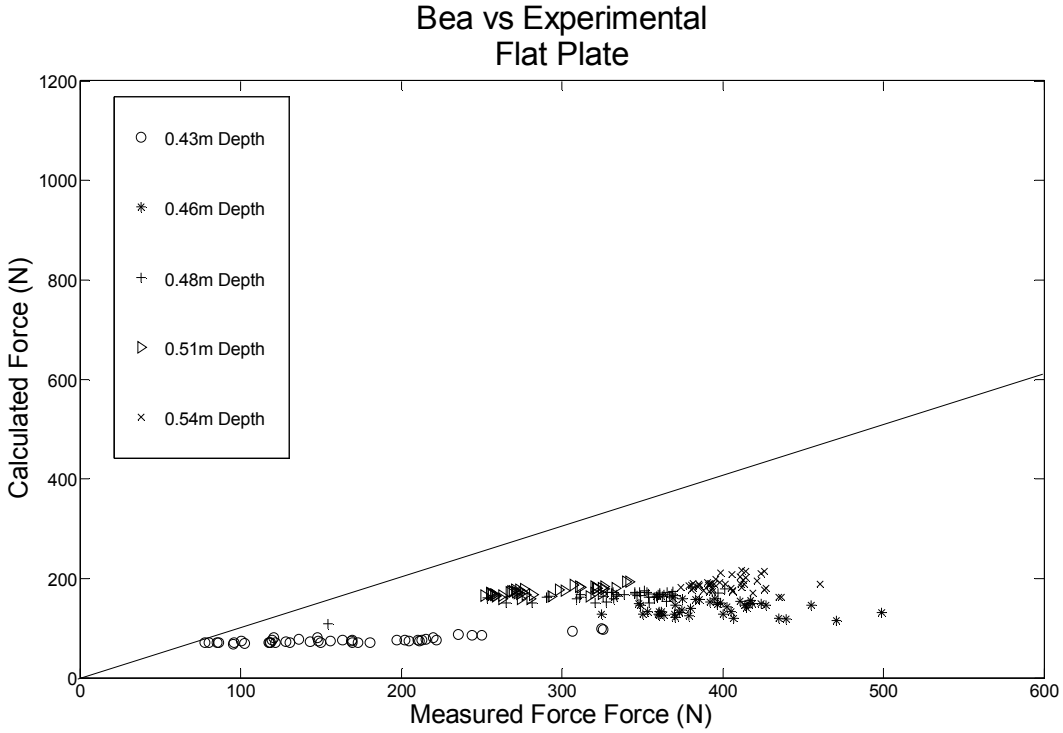

Figure 5- 5 Bea method compared to vertical force measurements

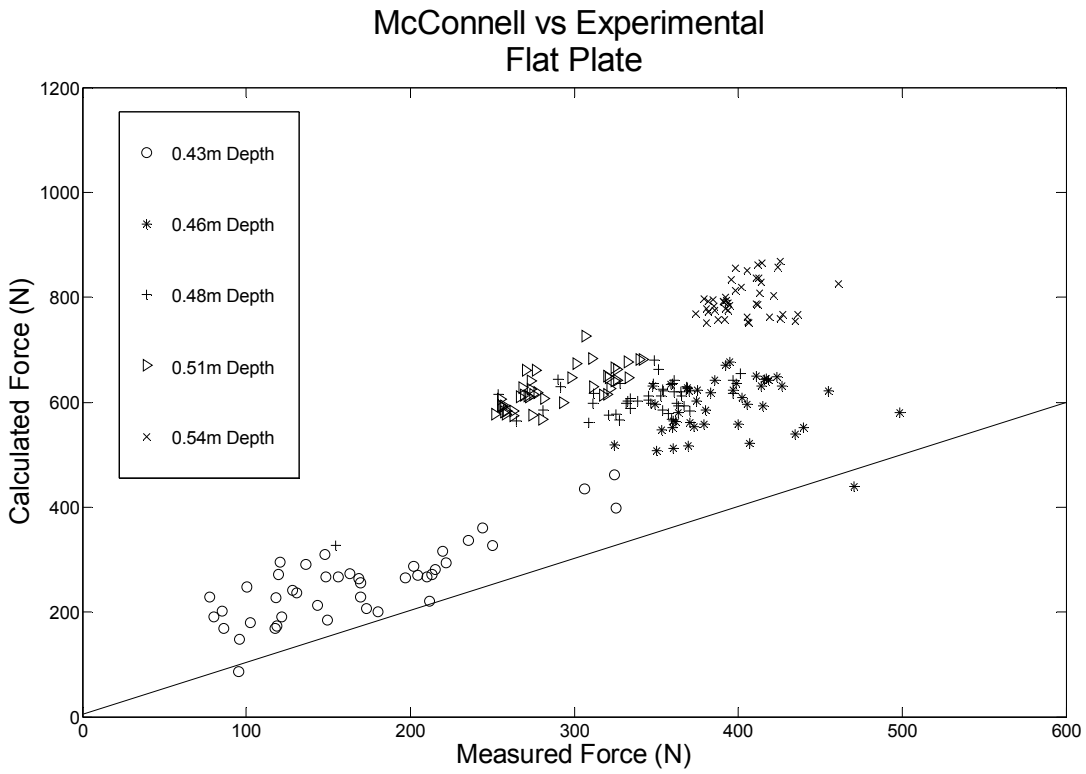

Figure 5- 6 McConnell method compared to vertical force measurements

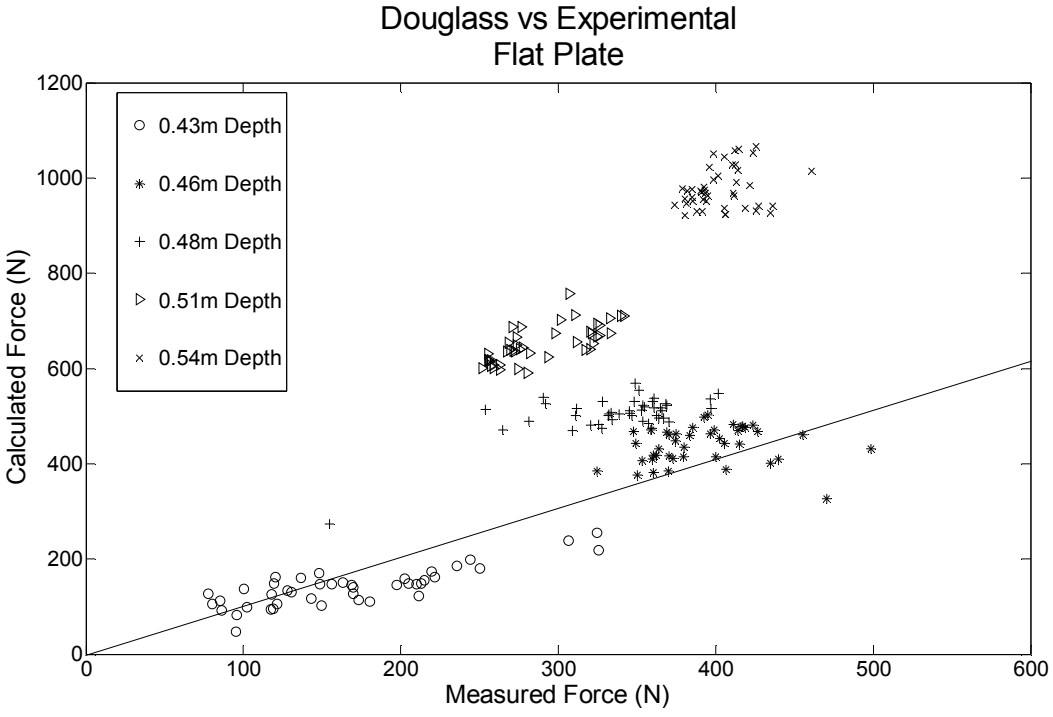

Figure 5- 7 Douglass method compared to vertical force measurements

Each point that is graphed represents the force produced by one wave event. On each figure, 5 tests with varying water depth are shown. The forces vary within the individual depths due to the non-uniform waves which were discussed in Chapter IV.

In general the hydrodynamic methods (Kaplan and Bea) tend to underestimate the vertical forces and the hydrostatic methods (McConnell and Douglass) tend to overestimate the vertical forces. No method showed a perfectly linear correlation with the measured vertical forces. The Douglass method in particular showed the best overall bias (measured vertical force mean divided by calculated vertical force mean) at lower water depths. Table 5-1 shows the vertical force bias for all four methods for individual water depths and overall as well the standard deviation for the overall bias. It is apparent that no method was able to sufficiently predict the change in vertical force due to water depth.

Table 5- 1 Previous methods vertical force statistical bias

Water Depth	Kaplan	Bea	McConnell	Douglass
0.43 m	1.585	2.190	0.652	1.180
0.46 m	2.104	2.800	0.663	0.890
0.48 m	1.571	2.060	0.560	0.669
0.51 m	1.111	1.674	0.463	0.444
0 54 m	1.280	2.140	0.506	0.413
Overall Bias	1.523	2.175	0.511	0.716
Standard Deviation	0.421	0.521	0.121	0.324

Comparing the measured horizontal forces to the existing methods similarly showed no perfect correlation. Figures 5-8 – 5-11 shows the four methods under investigation compared to horizontal measurements gathered during Experimental Set III. Again each point represents one wave event during a test. In each figure, 6 tests are shown representing different water depths. Table 5-2 shows the horizontal force bias for all four methods for individual water depths and overall as well the standard deviation for the overall bias.

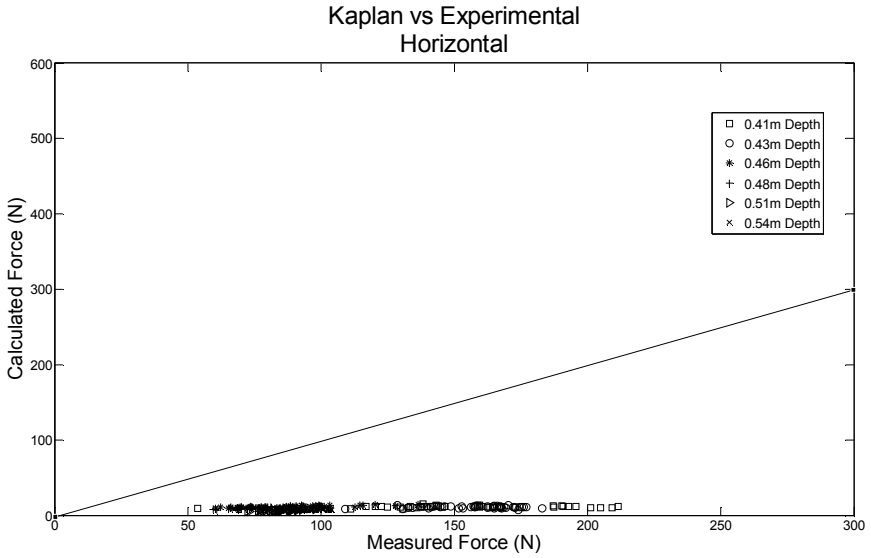

Figure 5- 8 Kaplan vs. experimental vertical force

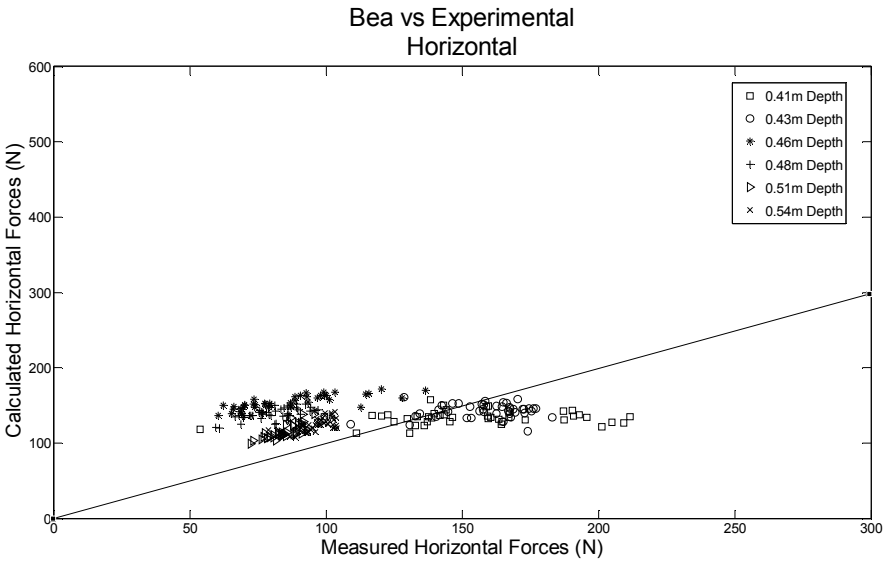

Figure 5- 9 Bea vs. experimental vertical force

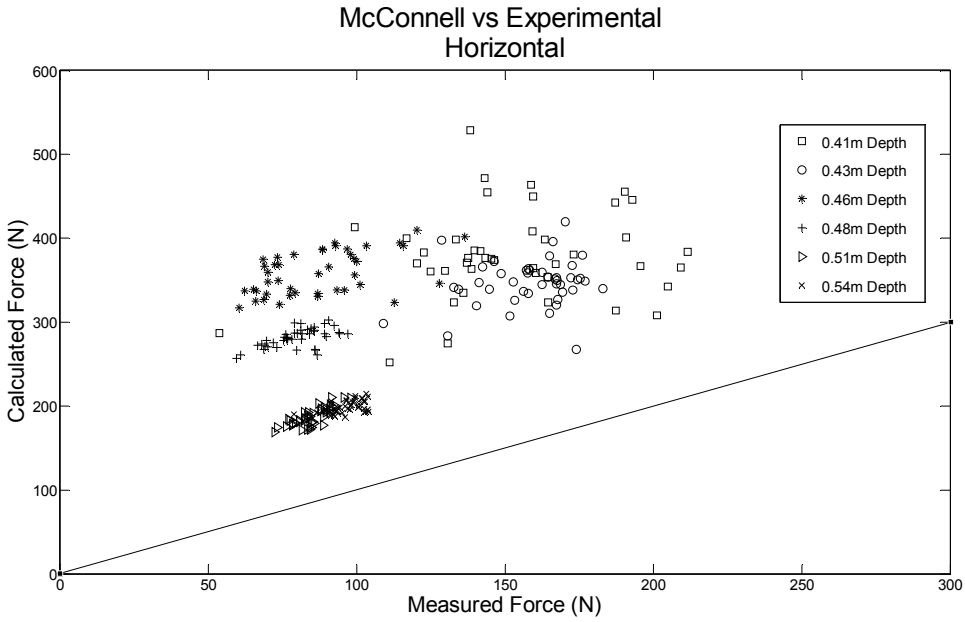

Figure 5- 10 McConnell vs. experimental vertical force

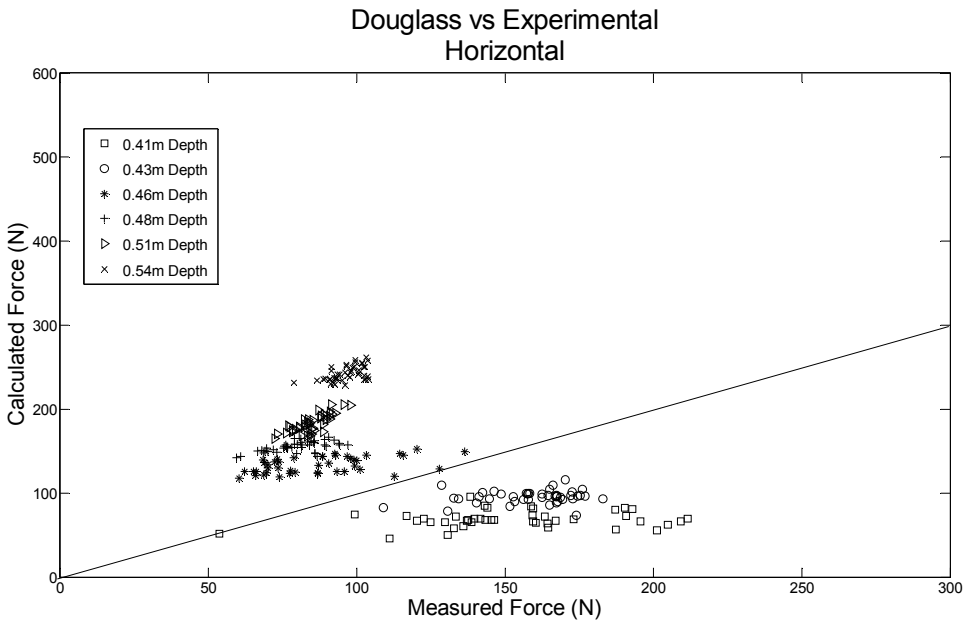

Figure 5- 11 Douglass vs. experimental vertical force

Table 5- 2 Previous methods horizontal force statistical bias

Depth	Kaplan	Bea	McConnell	Douglass
0.41 m	13.403	1.145	0.403	2.222
0.43 m	14.626	1.111	0.457	1.662
0.46 m	7.514	0.566	0.243	0.653
0.48 m	8.376	0.576	0.284	0.515
0.51 m	12.544	0.738	0.454	0.464
0.54 m	21.510	0.778	0.485	0.399
Overall Bias	11.6	1.05	0.389	0.99
Standard Deviation	3.23	0.3386	0.106	0.748

Solitary Wave Experiment

The solitary wave experiment provided a more definitive data set than the monochromatic wave experiments. The model bridge was used for the solitary wave experiment. The McConnell and Douglass methods were compared to the measured vertical and horizontal forces.

Figures 5-12 and 5-13 show the McConnell and Douglass methods compared to the measured vertical force for the solitary wave experiments. Each point represents one wave event (one solitary wave test). During Experimental Set V the water depths tested were 0.39m, 0.41m, 0.43m, 0.46m, 0.48m, 0.51m, and 0.54m and the wave heights tested were 0.1m, 0.12m, 0.14m, and 0.16m.

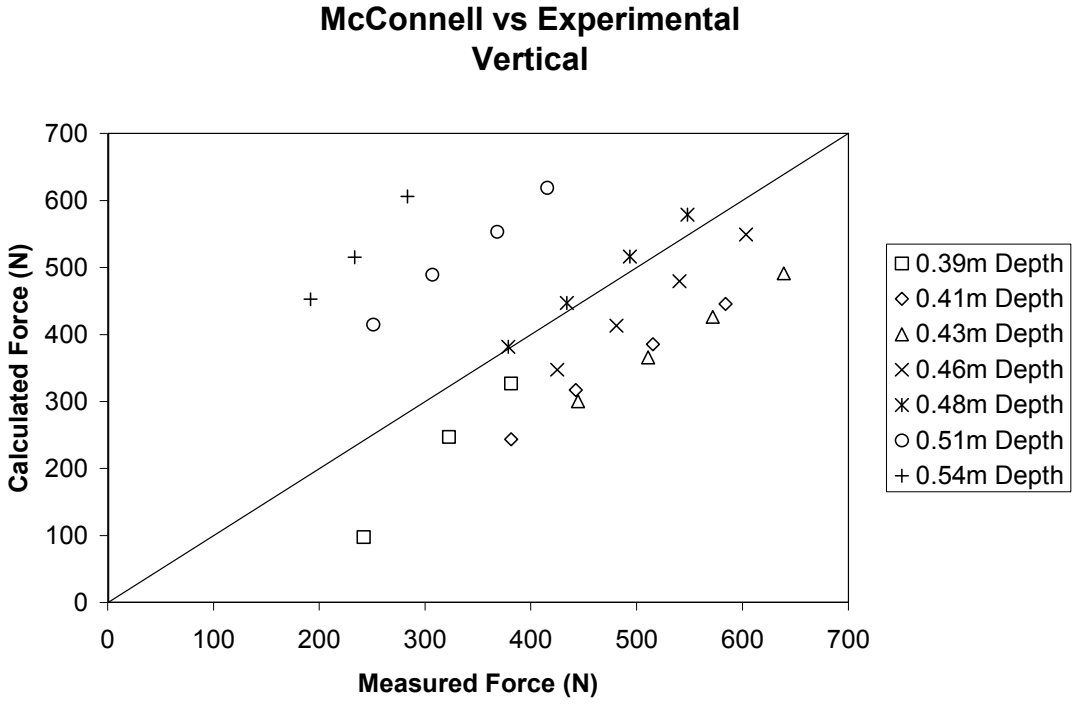

Figure 5- 12 McConnell vs. experimental vertical force solitary wave results

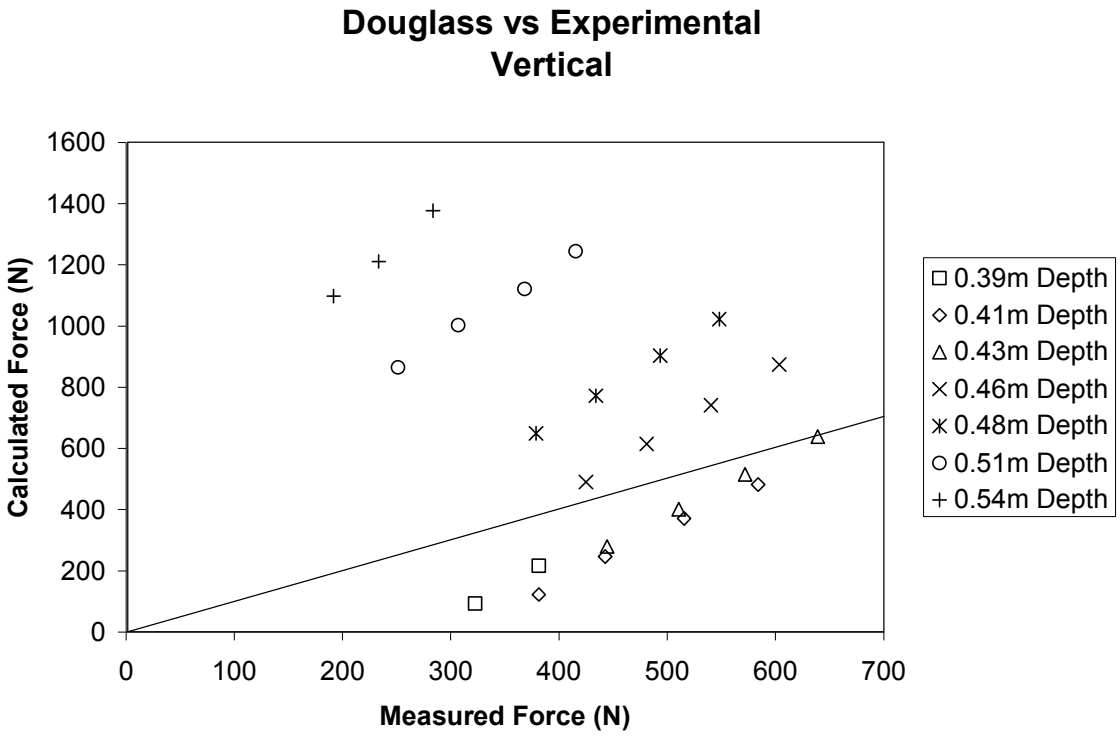

Figure 5- 13 Douglass vs. experimental vertical force solitary wave results

It can be observed that in both methods several points (tests) are overestimated. These points represent the tests carried out at higher water depths (h>0.48m). Recall from Figure 4-10 that as the water depth increased the vertical force raised linearly and peaked when the water depth reached the deck level. Neither method predicts this peak as the water depth increases.

Figures 5-14 and 5-15 show the McConnell and Douglass methods compared to measured horizontal force.

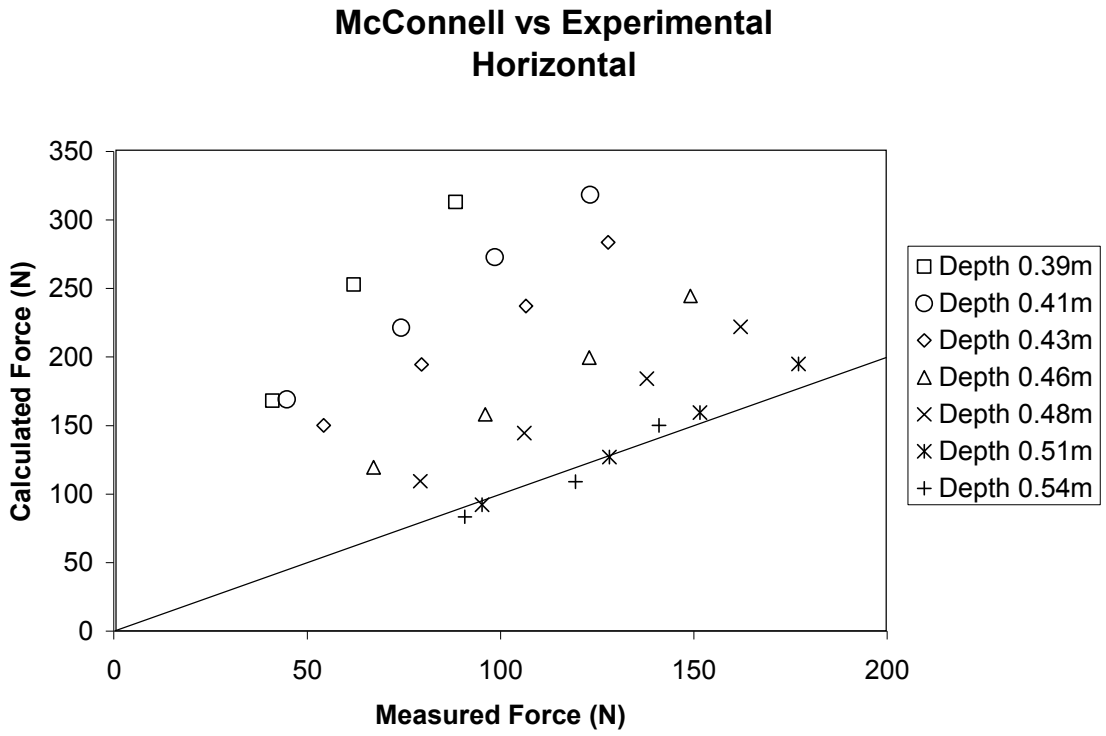

Figure 5- 14 McConnell vs. experimental horizontal force solitary wave results

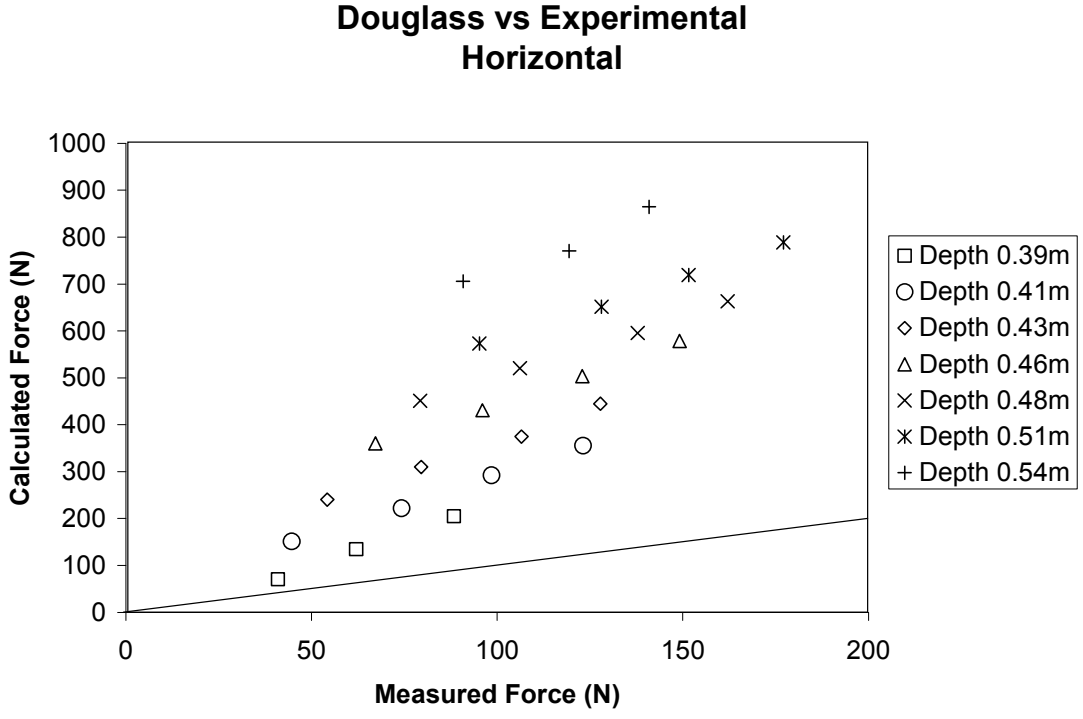

Figure 5- 15 Douglass vs. experimental horizontal force solitary wave results

Both methods overestimate the measured horizontal force. It appears the McConnell method increases in accuracy as the water depth increases. This trend is opposite to the Douglass prediction of the vertical force. The Douglass method increasingly over predicts the horizontal force as the water depth rises.

Conclusion of Previous Methods Comparison

None of the existing methods showed a perfect correlation with measured forces for all water depths tested. The hydrodynamic methods seemed to have less correlation compared to the hydrostatic methods. By observing the wave location when the maximum force occurs, a hydrostatic forcing is suggested.

CHAPTER VI

SUGGESTED METHOD

In chapter IV it was observed that the dominant forcing in both the vertical and horizontal direction is hydrostatic. No clear advantage was observed between the McConnell and Douglass methods. Thus, a suggested method for estimating forces on bridge structures is proposed herein. The Douglass method was used as a base for this suggested method due to its simplicity. The flat plate will first be discussed and used for developing the suggested method because of its simple geometry. Later, the effects of a complex geometry are discussed and force estimation methods are developed.

Wave Height and Vertical Force Correlation

A wave height correlation to vertical force is needed before continuing the development of the suggested method which is dominantly hydrostatic and only quasi-dependent on wave height. Hydrodynamic methods estimate forces on structures using fluid velocities and accelerations. These velocities and accelerations are direct functions of wave height among other parameters. The logic is that if the vertical force was dominantly dependent on hydrodynamic forcing then it should be linearly correlated to the wave height. The following figure is a plot of wave height versus vertical force from the data collected during the Experimental Set IV for several water depths. Each point represents a single wave event. The data is sorted by water depth. Within a water depth there is variation in wave heights due to non-uniform waves. Observing the 0.43m depth

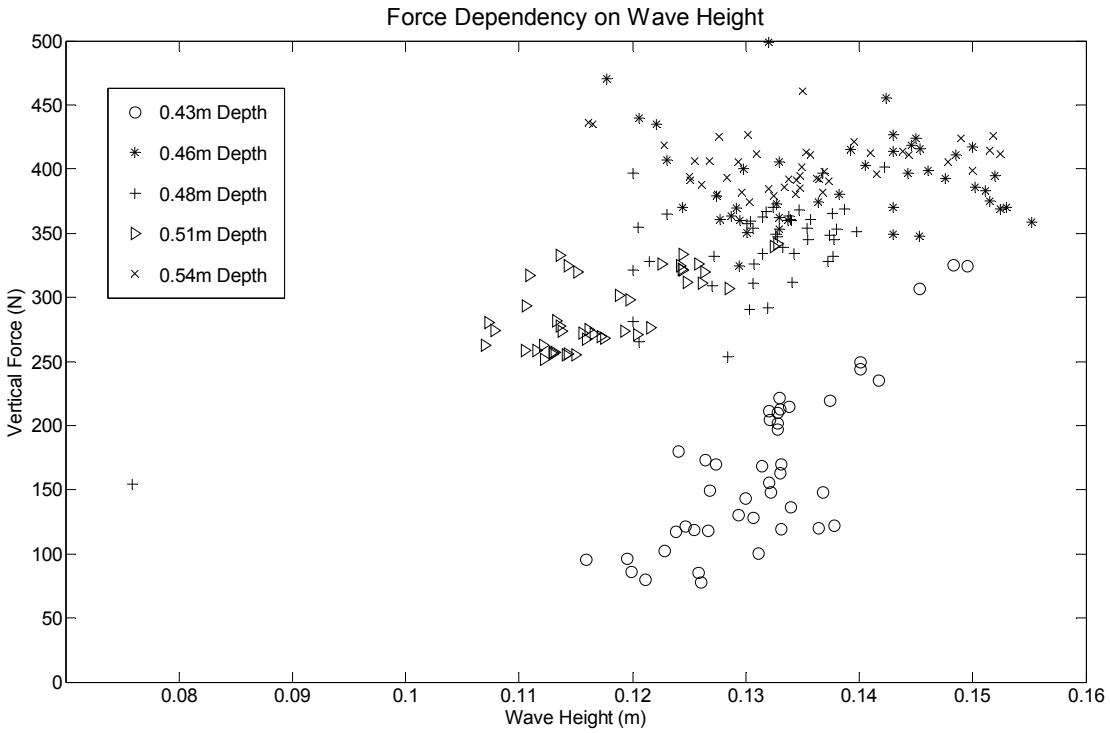

Figure 6- 1 Vertical force compared to wave height

visually a correlation exists between increased wave height and vertical force. However, as the depth increases the correlation becomes difficult to observe. Table 6-1 shows the correlation coefficient for each depth shown in Figure 6-1. The large scatter of data

Table 6- 1 Correlation coefficient for wave height compared to vertical force

Depth	0.43m	0.46m	0.48m	0.51m	0.54m
r	.8404	-0.0834	0.711	0.6742	0.05

makes it still difficult to discern any information about the correlation between wave height and vertical force. However, it appears as the water depth increases the correlation

decreases. This leads to the assumption that as water depth increases the wave height becomes less important.

Maximum Water Depth and Vertical Force Correlation

The maximum water depth is defined as the sum of the maximum η (wave crest elevation) and the water depth. Both hydrostatic methods reviewed calculated the vertical force without accounting for water to flow over the structure. It was observed visually that as a wave inundated the structure, the water would overtop or flow over the model if the wave crest was higher than the deck level.

If maximum water depth is plotted against vertical force, no obvious relationship exists. However, if the weight of the water that overtops the flat plate is added to the maximum vertical force a linear relationship is apparent. To quantify this, the overtopping water was simplified into a horizontal triangular column of water. The profile of this is shown in Figure 6-2. If the SWL is above the deck level the overtopping

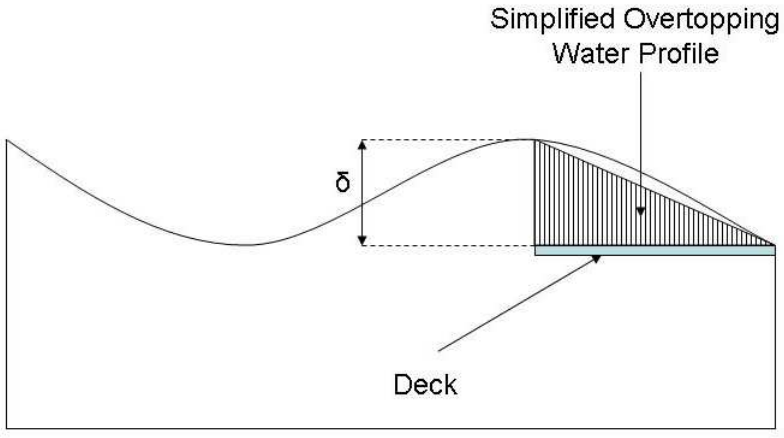

Figure 6- 2 Profile of overtopping water weight (lower water depth)

water weight is represented by a triangular column with the addition of a parallelepiped. The profile of this is shown in Figure 6-3. The equations for the weight of this simplified

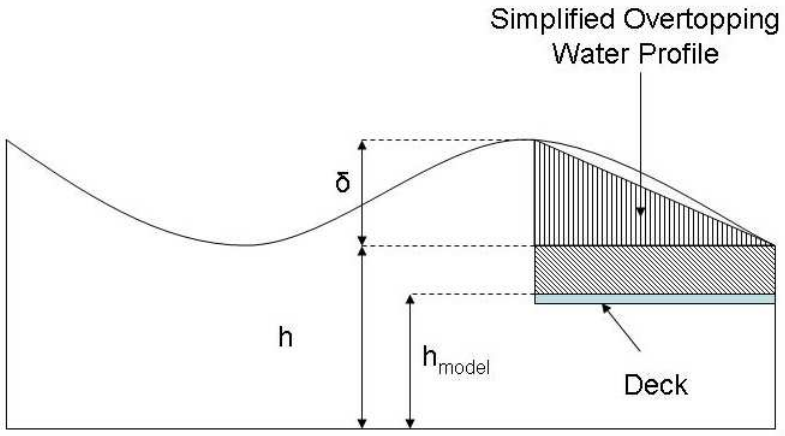

Figure 6- 3 Profile of overtopping water weight (higher water depth)

shape of overtopping water are given in the following equations.

$$F_w = \frac{1}{2}\gamma\delta A \qquad (6\text{-}1)$$

for h $\leq$ h_{model}

$$F_w = \frac{1}{2}\gamma\delta A + \gamma(h - h_{model})A \qquad (6\text{-}2)$$

For h > h_{model}

Where A is the wetted surface area of the flat plate.

Figure 6-4 shows the comparison of the modified vertical force (Vertical Force + Weight of Overtopping Water using equations 6-1 and 6-2) and maximum water height. The relationship is surprisingly linear and corresponds directly with Douglass (2006). The 0.43m data are not on the same line as the rest of the data because of the difference

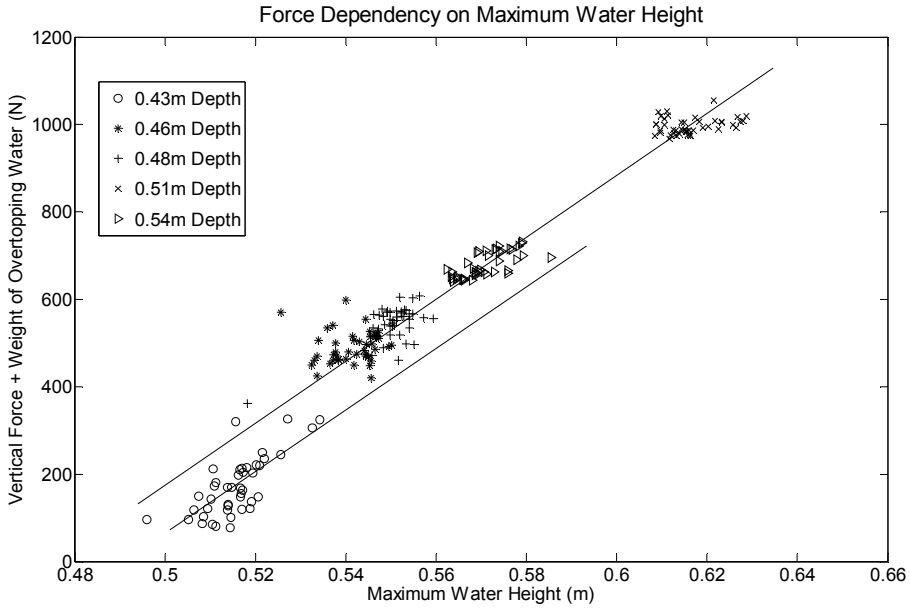

Figure 6- 4 Correlation of maximum wave crest above the SWL, η, and vertical force

in wetted surface area. At the depth of 0.43m the wetted surface area is not completely covered therefore it yields a lower upward force and follows a line shifted slightly down. The rest of the water depths' wetted surface area is equal to the surface area of the flat plate and consequently follow the same line.

Reversing the Correlation

The correlation between the maximum water height and vertical force clearly suggests a hydrostatic force behavior. If the previous method for determining the correlation of the maximum water height and vertical force were reversed, then a simple modified hydrostatic formula could estimate the vertical loads. The method the author suggests for calculating the vertical force on a flat plate is essentially the same as formulated in Douglass (2006) however the weight of the overtopping water would be

subtracted from the vertical force which the flat plate experiences. The suggested equation for estimating vertical force on a flat plate is shown in the following equation.

$$F_{vertical} = \gamma \delta A - F_w \qquad (6\text{-}3)$$

This method was used with the zero-upcrossing analysis to estimate the vertical forces from each wave crest. The estimated forces were then compared to the measured force resulting from the corresponding wave crest. Figure 6-5 shows the comparison of the empirical solution and the experimental measurements.

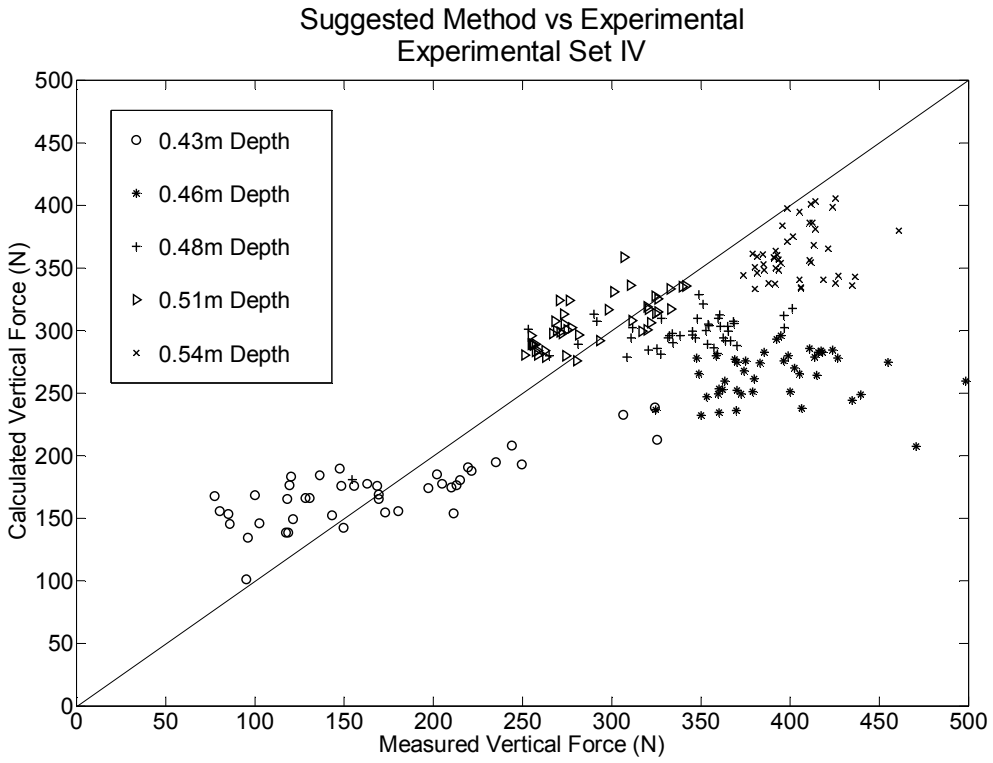

Figure 6- 5 Suggested method compared to measured vertical force on a flat plate

If the bias for each point (measured divided by calculated) is averaged, then the overall bias is 1.14 with a standard deviation of 0.251. There is still a great deal of

scatter, however this is somewhat to be expected due to the oversimplification of the force estimation.

Estimating Uplift Force for a Complex Geometry

It is important to be able to predict the forces on a complex geometry since the structures under investigation are highway bridges and not simple flat plates. The following outlines how the suggested method is modified to predict vertical forces on more complex geometries such as the bridge model. The actual theory behind estimating the uplift forces on a structure is simple. The total force equals the sum of the buoyancy of the inundated bridge and hydrostatic uplift minus the weight of the overtopping water. However, accurately calculating this can be complex if a great deal of accuracy is desired. For a structure with girders air-entrapment needs to be factored into the inundated bridge buoyancy term.

A visual way of understanding how the forces act on a structure is by "freeze framing" the inundating wave just when the wave crest reaches the leading edge of the structure. The hydrostatic uplift force is caused by the difference in elevation between the wave crest and the deck. The buoyancy force is caused by the amount of volume the bridge is displacing. If the SWL is below the deck level the buoyancy force needs to incorporate the volume displaced by air entrapment between the girders. The downward overtopping force is caused by the weight of the water on the deck.

Figure 6-6 shows a schematic of the forces acting on typical bridge deck when the SWL is at or below deck level. It should be noted that the hydrostatic force in this schematic incorporates the simplified overtopping water weight. From visual

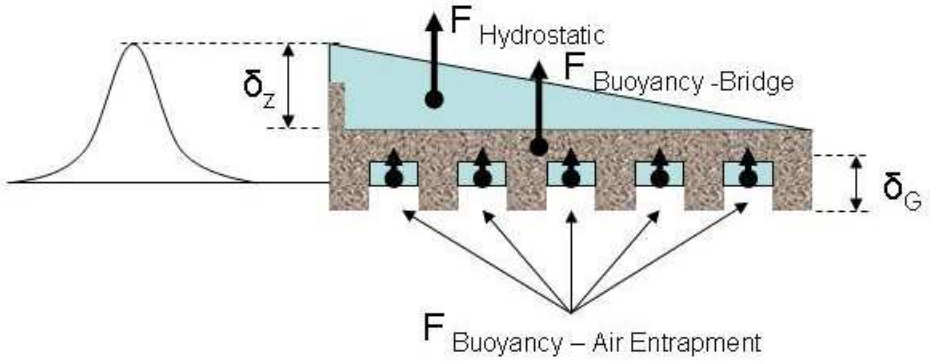

Figure 6- 6 Vertical force schematic for complex geometry

observations it was seen that the amount of air entrapped between girders is not constant and is never 100% of the total volume between the girders. The buoyancy from these girders is estimated by taking one half the maximum volume between the girders. The equations used to find these forces are as follows:

$$F_{Total} = F_{Hydrostatic} + F_{Bridge} + F_{AirEntrapment} \quad (6\text{-}4)$$

$$F_{Hydrostatic} = \gamma \delta_z A - F_w \quad (6\text{-}5)$$

$$F_{Bridge} = \gamma Vol_{Bridge} \quad (6\text{-}6)$$

$$F_{AirEntrapment} = (n-1)\frac{1}{2}\gamma \delta_G A_G \quad (6\text{-}7)$$

Where n is the number of girders.

The forces acting on the structure when the SWL is at or above the deck level change. Buoyancy from air-entrapment is no longer considered. The hydrostatic force is still calculated the same way and increases as the water depth increases. However, at the same time the overtopping water weight also increases as the water depth increases, which at a certain depth peaks the total force.

The following figures show this method compared to the forces calculated during the monochromatic bridge tests from Experimental Set I and III respectively. Each point on the figures represents a single wave event. Figure 6-7 is separated into various wave heights and water depths with a constant period of 1.8s. Figure 6-8 is separated into varying water depths. The overall bias for the suggested method compared to Experimental Set I is 1.056 with a standard deviation of 0.192. The overall bias for the suggested method compared to Experimental Set III is 0.969 with a standard deviation of 0.154. These figures show repeatability in both the experiments and the suggested method. It is clear from these figures that the dominant forcing is hydrostatic. However, a significant amount of scatter is still present.

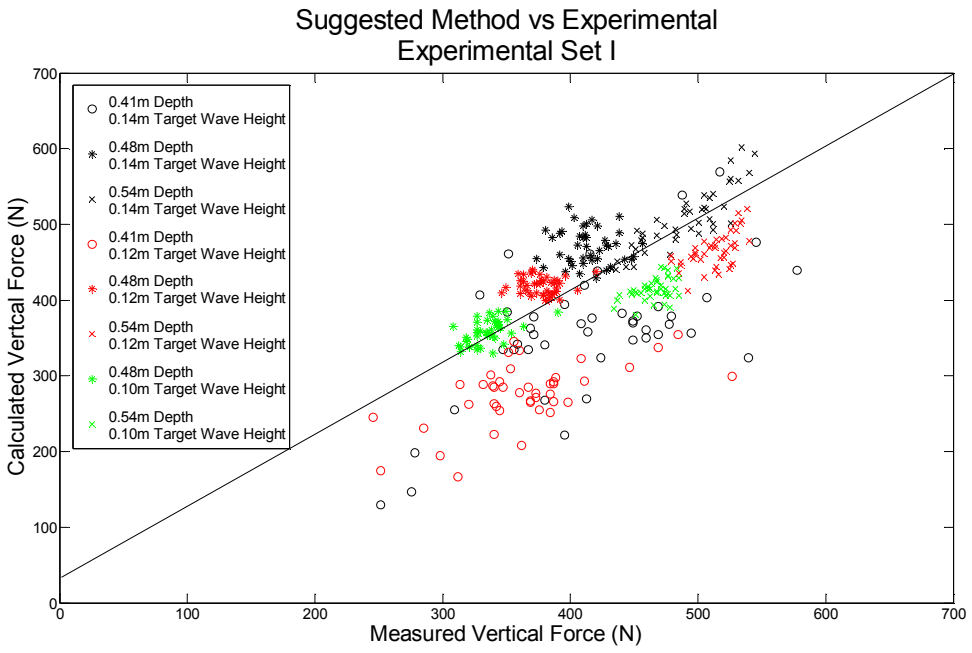

Figure 6- 7 Suggested method vs. measured vertical force (experimental set I)

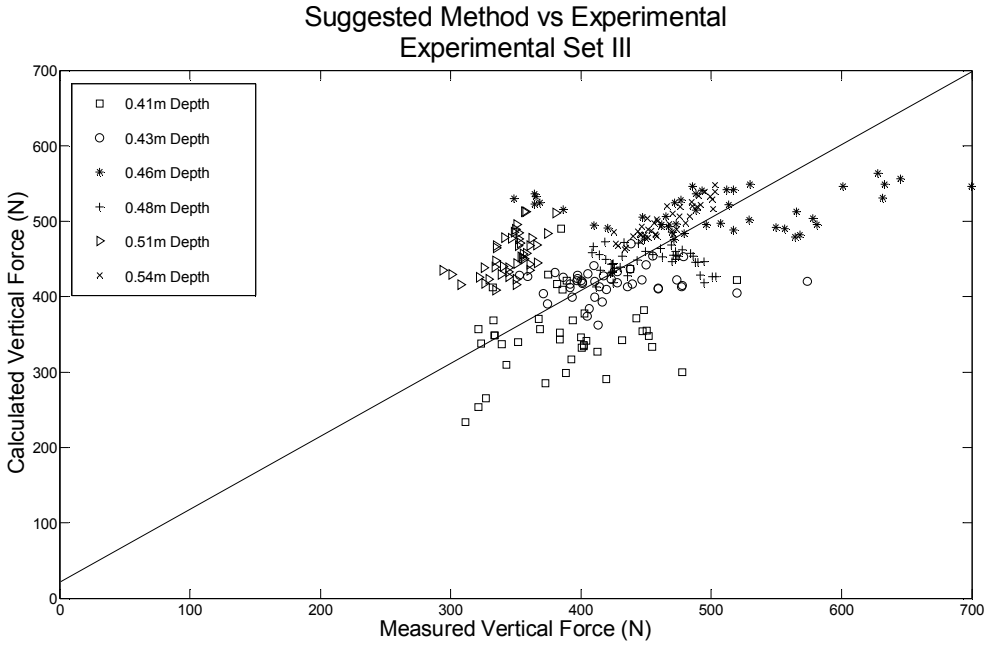

Figure 6- 8 Suggested method vs. measured vertical force (experimental set III)

Solitary Wave Comparison

The suggested method was applied to the solitary wave experiment. The more discernable data produced from the Experimental Set V gives an indication of the validity of the suggested method. Figure 6-9 shows vertical force calculated using the suggested method compared to the measured data from Experimental Set V. The overall bias for the suggested method compared to Experimental Set V is 0.849 with a standard deviation of 0.83. It can be observed from the comparison plot that the suggested method tends to over estimate the measured vertical velocities. Recall that these calculations are done using an oversimplified model of the wave impacting the structure "freeze-framed" when the wave crest is located at the leading edge. If the overtopping weight is increased from the 0.5 factor to 0.65 factor a better relationship is seen. This is shown in Figure 6-10. The overall bias when modifying the overtopping weight for the vertical suggested

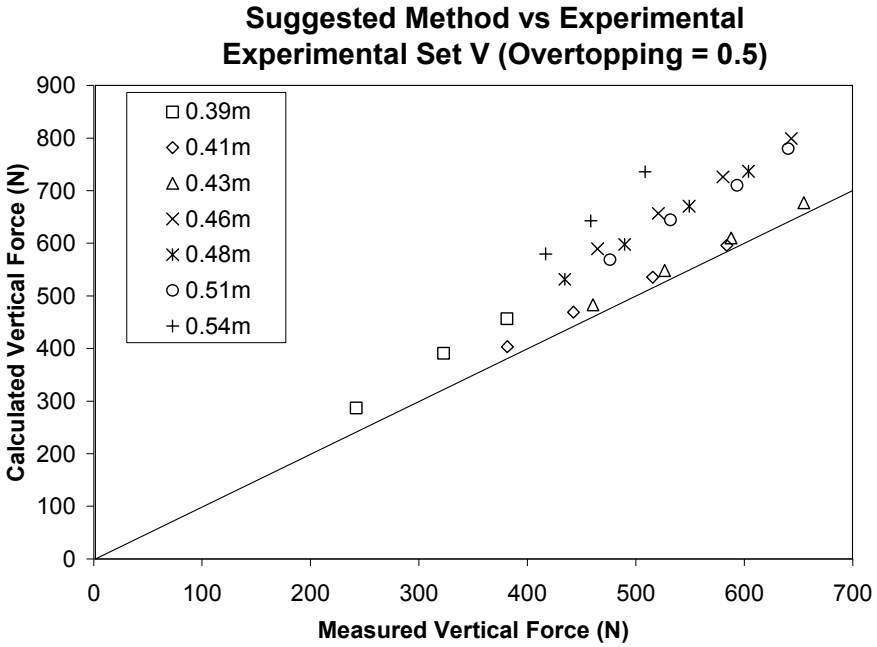

Figure 6- 9 Suggested method vs. measured vertical force (experimental set V)

method compared to Experimental Set V is 0.925 with a standard deviation of 0.077.

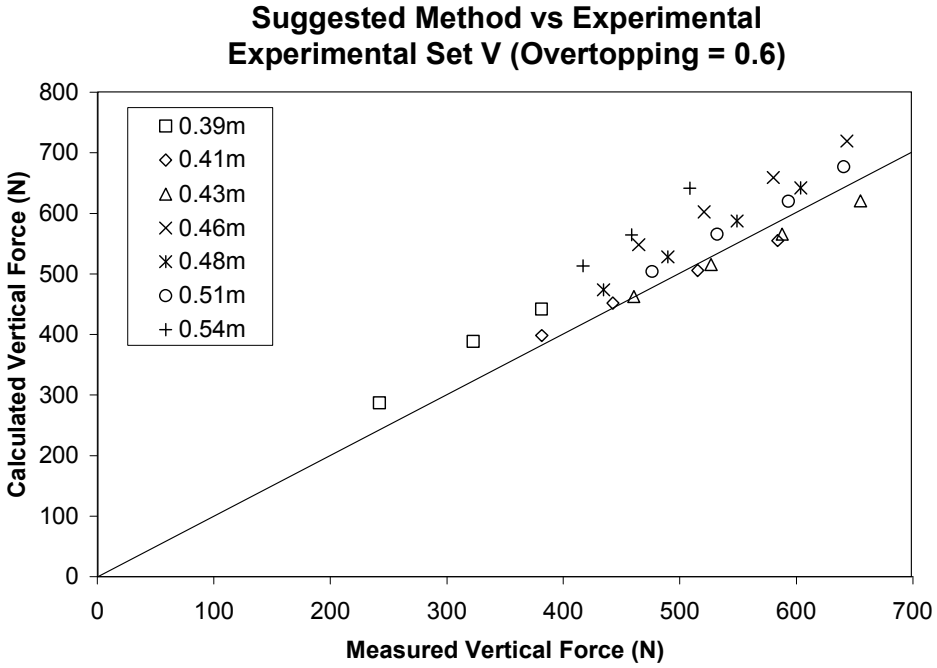

Figure 6- 10 Suggested method vs. measured vertical force with modified overtopping (experimental set V)

To demonstrate the increase in overtopping weight, refer to Figure 6-11. Computation of the original overtopping weight uses a simple horizontal triangular column or combination of a horizontal triangular column and parallelepiped to represent the water flowing over the top of the structure. It is speculated the actual weight of the overtopping water is greater than that represented by the simple triangular column. This justifies slight alterations in the overtopping weight done in Figure 6-9 to create a better relationship.

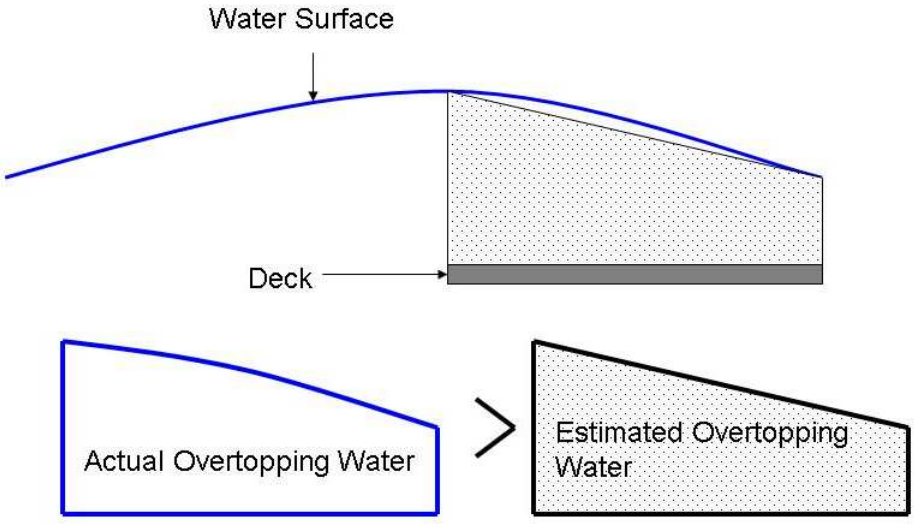

Figure 6- 11 Schematic of realistic overtopping weight

Suggested Method for Calculating Horizontal Forces

As discussed in Chapter V the measured horizontal force was found from the solitary wave experiment to increase linearly. The Douglass method increased linearly, but substantially overestimated the force. Again for developing a horizontal suggested method the Douglass method was used as a base.

The Douglass method did not include the overtopping water weight for the vertical force method which caused the method to overestimate the vertical force in higher water depths. Using similar logic, the Douglass method also did not include the hydrostatic force of the water on the backside of the structure when calculating the horizontal force. Incorporating this and eliminating the girder addition to the horizontal force when the SWL was above the structure essentially makes up the new suggested method for horizontal force.

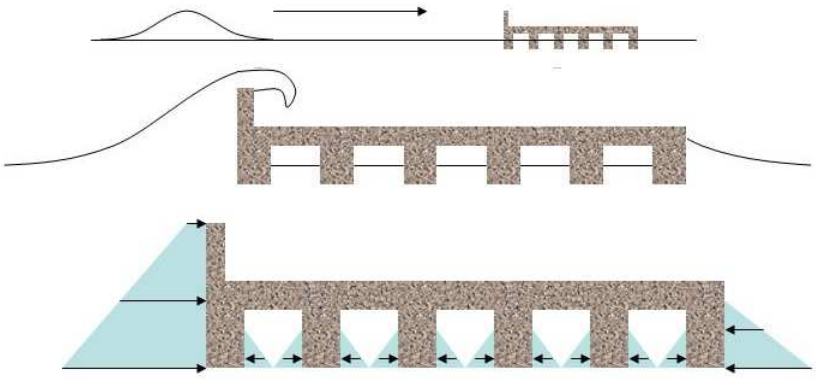

Figure 6- 12 Horizontal force suggested method schematic

It is important to emphasis that the hydrostatic force on the backside of the structure only exists when the SWL is above the girder level. Figure 6-12 shows a force diagram schematic of representing the new method. The horizontal suggested method in equation form is as follows.

$$F_{Total} = F_{Hydrostatic\_Front} + F_{Hydrostatic\_back} \tag{6-8}$$

$$F_{Hydrostatic\_Front} = 0.5 * \left(\eta_{\max} + h - h_{girders}\right) H_{bridge} L_{bridge} \gamma \tag{6-9}$$

Where $\eta_{max} < h_{deck}$

$$F_{Hydrostatic\_Front} = 0.5 * \left[\left(\eta_{\max} + h - h_{girders}\right) + \left(\eta_{\max} - h_{deck}\right)\right] H_{bridge} L_{bridge} \gamma \tag{6-10}$$

Where $\eta_{max} > h_{deck}$

$$F_{Hydrostatic\_back} = 0 \tag{6-11}$$

Where SWL < $h_{girders}$

$$F_{Hydrostatic\_back} = 0.5(h - h_{girder})^2 L_{bridge}\gamma \tag{6-12}$$

Where SWL > $h_{girders}$

Figure 6-13 is a definition sketch of the terms used in Equations 6-8 to 6-12.

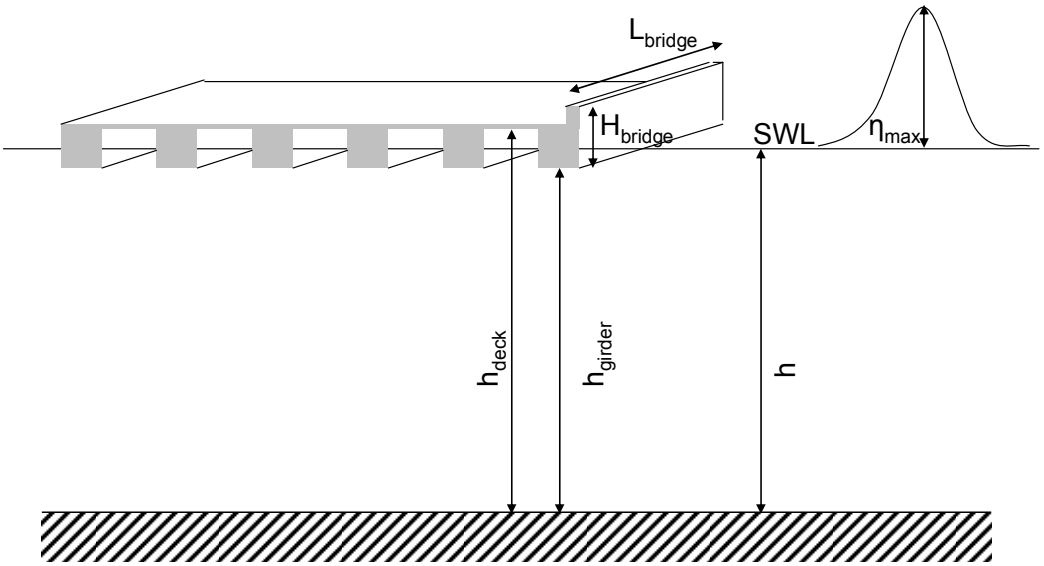

Figure 6- 13 Definition sketch for horizontal force suggested method

The suggested horizontal method was compared to the solitary wave measured horizontal forces. Figure 6-14 shows the suggested method horizontal force calculation compared to the measured data from Experimental Set V. The overall bias for the horizontal suggested method compared to Experimental Set V is 0.949 with a standard deviation of 0.124.

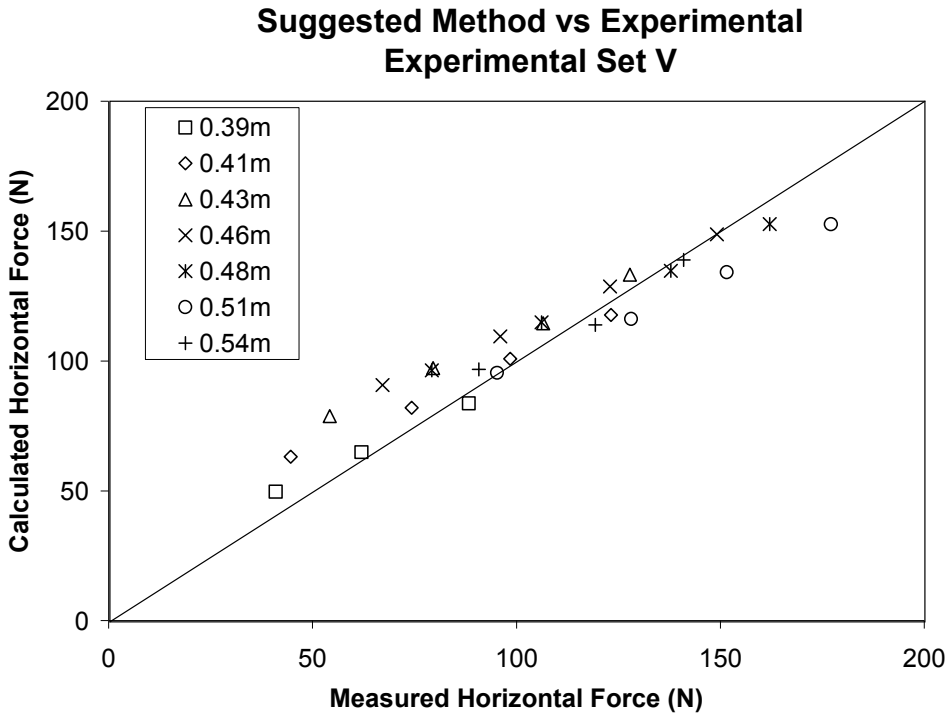

Figure 6- 14 Suggested method vs. measured horizontal force (experimental set V)

As opposed to the Douglass method where the horizontal prediction severely overestimated the measured forces, the new method has reduced the predicted force by subtracting the hydrostatic force caused by the water on the backside of the structure when the SWL was above the girders.

Hydrodynamic Consideration

The suggested method is based on the hydrostatic forcing method. The method was developed by essentially "freeze-framing" the wave as it impacted the bridge and summing all of the forces. However, in reality the wave is in motion and therefore the water particles are in motion. Therefore, hydrodynamic effects are still present during a wave event.

Using linear theory, wave particle velocities and accelerations were calculated for sample wave conditions. They were then used to calculate vertical and horizontal forces using the Morison equations (Morison et al., 1950) used in the Bea method (excluding slamming) by integrating along the appropriate area of the model. However, differing from the Bea method, the forces were calculated when wave crest approached the leading edge of the model as observed from the measured data. When this was done, force calculations were found to be on the order of the error associated with the suggested method.

Table 6- 2 Hydrostatic contribution example

Wave Height (H)	Wave Period (T)	Water Depth (h)
14cm	1.8s	48cm
Hydrodynamic Contribution	Buoyancy Contribution	Total Vertical Force
~15N	85N	~525 +/-20N

Table 6-2 demonstrates the hydrodynamic contribution for a sample wave on the flat plate model. The hydrodynamic contribution was calculated using the Bea method (excluding slamming) when the wave crest approaches the leading edge of the structure. The total force is the measured value from Experimental Set IV. This value and the error (scatter) can be seen visually in Figure 6-14. The dynamic contribution is significantly smaller than the total vertical force even if the buoyancy is removed.

In conclusion, hydrodynamic forces are present during a wave event however at the moment of maximum force, the hydrostatic component is dominant. When the

hydrodynamic force is greatest, the wave has already inundated the structure and the total force is less than when the wave crest first approached the leading edge.

Biloxi Case Study

Douglass et al. 2006 presents a case study of the U.S. 90 highway bridge over the Biloxi Bay. During Hurricane Katrina the U.S. 90 Bridge crossing the Biloxi Bay, Mississippi sustained an extreme amount of damage due to increased water depth and waves. Douglass et al. (2006) uses this case study to demonstrate the application of their recommended methodology. Using the same bridge and storm information presented by Douglass et al. (2006), the suggested method is applied.

An actual bridge span of the Biloxi Bay Bridge is relatively complex. It can be simplified, however, into several blocks of different dimensions making the sample calculations significantly easier. This simplified model is shown in Figure 6-15.

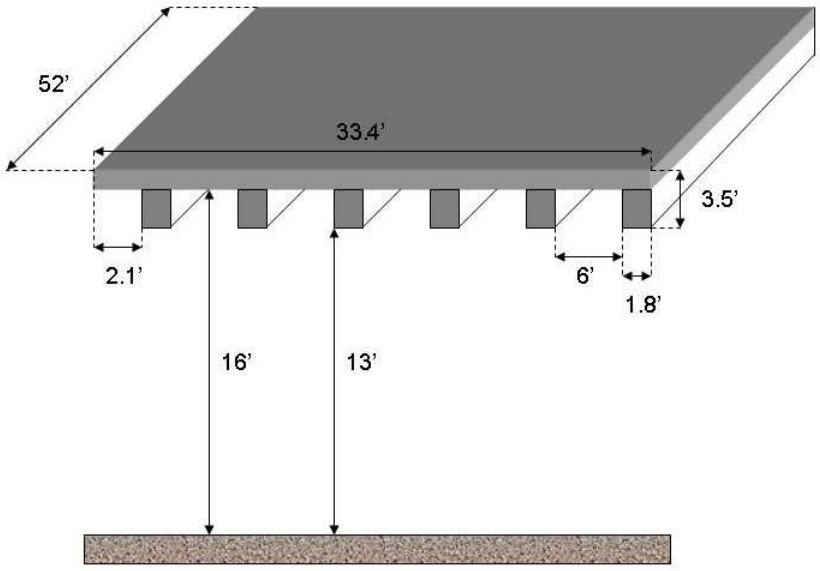

Figure 6- 15 U.S. 90 highway bridge over Biloxi Bay simplified schematic

The SWL and η_{max} provided in the literature are 11.9ft and 8.06ft respectively. The following calculates the vertical and horizontal forces using the suggested method.

Vertical Force

The vertical force equations and calculations are listed below.

$$F_{Total} = F_{Hydrostatic} + F_{Bridge} + F_{AirEntrapment} \tag{6-13}$$

$$F_{Hydrostatic} = \gamma \delta_z A - F_w \tag{6-14}$$

$$F_{Bridge} = \gamma Vol_{Bridge} \tag{6-15}$$

$$F_{AirEntrapment} = (n-1)\frac{1}{2}\gamma \delta_G A_G \tag{6-16}$$

$$F_w = 0.5\gamma \delta_z A$$

$$F_w = 0.5 * 62.4 * \left(\left(11.9 + 8.06\right) - 16.5\right)\left(52 * 33.4\right) = 187{,}491 lbs$$

$$F_{Hydrostatic} = 62.4\left(\left(11.9 + 8.06\right) - 16.5\right)\left(52 * 33.4\right) - 187{,}491 = 187{,}491 lbs$$

$$F_{Bridge} = 62.4\left(\left(33.4 * 52 * .5\right) + 6\left(1.8 * 3 * 52\right)\right) = 159{,}319 lbs$$

$$F_{AirEntrapment} = (6-1)\frac{1}{2}62.4 * 3 * 6 * 52 = 146{,}016 lbs$$

$$F_{Total} = 187{,}491 lbs + 159{,}319 lbs + 146{,}016 lbs = 492{,}826 lbs = 246.4 tons$$

Horizontal Force

The horizontal force equations and calculations are listed below.

$$F_{Total} = F_{Hydrostatic\_Front} + F_{Hydrostatic\_back} \tag{6-17}$$

$$F_{Hydrostatic\_Front} = 0.5 * \left[\left(\eta_{\max} - h_{girders}\right) + \left(\eta_{\max} - h_{deck}\right)\right] H_{bridge} L_{bridge} \gamma \tag{6-18}$$

$$F_{Hydrostatic\_back} = 0 \tag{6-19}$$

$$F_{Hydrostatic\_Front} = 0.5 * \left[\left(8.06 + 11.9 - 13\right) + \left(8.06 + 11.9 - 16\right)\right] 3.5 * 52 * 62.4 = 62{,}008 lbs = 31.0 tons$$

$F_{Total} = 62{,}008lbs = 31.0tons$

The predicted vertical and horizontal force using the suggested method is 493,000lbs and 62,000lbs respectively. Douglass et al. (2006) method predicts the vertical and horizontal forces to be 440,000lbs and 230,000lbs. The vertical force predictions for the two methods are very similar. This is to be expected since the suggested method does not differ greatly from the Douglass method until the SWL comes above the deck level.

CHAPTER VII

CONCLUSION

Research was conducted to investigate wave and surge forces on deck structures. Two physical models, a 1:20 bridge model and flat plate were used during the experimentation. Varied wave conditions and water depths were tested on both physical models. Force and wave measurements and visual data were recorded. The data were then analyzed and force mechanisms and trends were investigated. The goal of this research was to evaluate a method to estimate wave and surge loads on bridge decks given a specific wave condition.

Four preexisting theoretical methods for calculating forces on deck-like structures were compared to the measured force data from the experiments. The literature for the selected methods under investigation include Kaplan et al. (1995), Bea et al. (2001), McConnell et al. (2004), and Douglass et al. (2006). The following conclusions were made from the comparisons:

- No method under review sufficiently predicted the measured forces for all wave conditions
- Both the Kaplan and Bea methods which are based on hydrodynamic theory consistently underestimated the forces.
- Both the McConnell and Douglass methods which are based on hydrostatic theory in general overestimated the forces, especially at a SWL above or at deck level.
- The Douglass method provided the best relative correlation for uplift forces for a SWL below the deck elevation.

Due to the unsatisfactory prediction of the preexisting methods, the forcing events were investigated in greater detail to better understand the damaging mechanisms during a wave event. After reviewing force events, it was observed that the maximum vertical force occurred as the crest of the wave approached the leading edge of the structure. It was also observed that the maximum horizontal force occurred at the same time as the maximum vertical force when the SWL was below the deck level. When the SWL was above the deck level and structure was then fully submerged the maximum horizontal force was slightly delayed in reference to the vertical force. In the hydrostatic theories developed by Douglass and McConnell it can be determined that the maximum force will occur when there is the greatest difference in the water immediately in front of the structure and the structure itself. This corresponds to the experimental observations.

In contrast, in the hydrodynamic theories developed by Kaplan and Bea the maximum force will occur when the wave crest has reached close to the middle of the structure. Also, using underwater video cameras, it was observed that air was trapped between girders when the SWL was below the deck level. This leads to the following conclusions:

- The dominant uplift force mechanism is caused by hydrostatic pressure differences when the wave crest reaches the leading edge of the structure.
- Air-entrapment does exist between girders when the SWL is below the deck in experimental tests. Air-entrapment has the potential to contribute a significant uplift buoyancy force.

Using the Douglass method for calculating forces on bridges decks as a base, an improved method was developed. The improved method includes uplift forces incurred by overtopping water and air-entrapment. It was found that adding the buoyancy effects for air-entrapment and the downward force of overtopping created the non-linear variation in vertical force as the water depth varied observed in the measured data. The improved method also includes lateral forces incurred by stabilizing hydrostatic forces on the trailing edge of the structure when the SWL is above the girder level. It was found that adding the opposing hydrostatic force on the trailing edge of the structure reduced the over-estimation from the Douglass method. Incorporating these effects for both vertical and horizontal forces, significantly improved the correlation between the experimental results and calculated forces.

Hydrodynamic effects were also investigated. Using linear theory and the Morrison theory used by Bea and Kaplan, it was found that the force contribution from the hydrodynamic forces when the wave crest approached the leading edge (location of maximum uplift force) was of the same order of the error associated with using the hydrostatic theory. This leads to the following conclusions:

- Hydrodynamic force accompanies the hydrostatic force in the overall hydraulic loading of the structure.
- The hydrodynamic contribution to the maximum force is significantly less than the hydrostatic contribution.

REFERENCES

Bea, R. G., Xu, T., Stear, J., and Ramos, R. (2001). "Wave Forces on Decks of Offshore Platforms." *Journal of Waterways, Port, Coastal & Coastal Engineering,* ASCE, 125(3), 136-144.

Cruz-Castro O., Edge B., and Douglass S. (2006). "Hurricane Forces Measurements on Bridge Decks." *Proceedings of the Conference on the Application of Physical Modeling to Port and Coastal Protection*, Portugal, 83-86.

Dean, R. G., and Dalrymple, R. A. (2002) *Coastal processes: with engineering application.* Cambridge University Press, New York.

Douglas, S., Chen, Q., Olsen, J., and Edge, B. (2006)."Wave Forces on Bridge Decks." *U.S Department of Transportation Report*, Federal Highway Administration, McLean, VA.

Kaplan, P., (1992). "Wave Impact Forces on Offshore Structures: Re-examination and New Interpretations." *Offshore Technology Conference Paper 6814, 24th Offshore Technology Conference*, Houston, 79-98.

Kaplan, P., Murray, J.J., and Yu, W.C. (1995). " Theoretical Analysis of Wave Impact Forces on Platform Deck Structures." *Proceedings of the 14th International Conference on Offshore Mechanics and Arctic Engineering,* Copenhagen, Denmark, 1(A), 189-198.

Kerenyi, K (2005). "Wave Forces on Bridge Decks." *U.S. Dept. of Transportation Technical Note,* Federal Highway Administration, McLean, VA.

McConnell, K., Allsop, W., and Cruickshank, I. (2004). *Piers, jetties, and related structures exposed to waves: Guidelines for hydraulic loadings*. Thomas Telford Press, London.

Morison, J.R., O'Brien, M.P.O., Johnsen, J.W., and Schaff, S.A., (1950). "The Forces Exerted by Surface Waves on Piles." *Petrol Trans*., 189, 149-157.

Padgett, J., DesRoches, R., Nielson, B., Yashinsky, M., Kwon, O., Burdette, N., and Tavera, E. (2008). "Bridge Damage and Repair Costs from Hurricane Katrina." *Journal of Bridge Engineering*, 13(1), 6-14 .

Sarpkaya, T., and Isaacson, M., (1981), *Mechanics of wave forces on offshore structures*. Van Nostrand Reinhold, New York.

Tirindelli, M., McConnell, K., Allsop, N.W.H., and Cuomo, G., (2002). "Exposed jetties: inconsistencies and gaps in design methods for wave-induced forces." *Proceedings of the 28th ICCE,* Cardiff, UK*,* 1684-1696.

VITA

Name: Ronald Lee McPherson

Address: 2836 Las Campanas, Farmers Branch, TX 75234

Email Address: rlmcpher@tamu.edu

Education: B.S., Aerospace Engineering, Texas A&M University, 2006